Eur. Phys. J. E **14**, 17–34 (2004)
DOI 10.1140/epje/i2003-10089-3

THE EUROPEAN PHYSICAL JOURNAL E

Stretching of semiflexible polymers with elastic bonds

J. Kierfeld[1,a], O. Niamploy[1,2], V. Sa-yakanit[2], and R. Lipowsky[1]

[1] Max-Planck-Institute of Colloids and Interfaces, 14424 Potsdam, Germany
[2] Forum for Theoretical Science, Department of Physics, Faculty of Science, Chulalongkorn University, Bangkok 10330, Thailand

Received 7 October 2003 and Received in final form 4 March 2004 /
Published online: 26 May 2004 –

Abstract. A semiflexible harmonic chain model with extensible bonds is introduced and applied to the stretching of semiflexible polymers or filaments. The semiflexible harmonic chain model allows to study effects from bending rigidity, bond extension, discrete chain structure, and finite length of a semiflexible polymer in a unified manner. The interplay between bond extension and external force can be described by an effective inextensible chain with increased stretching force, which leads to apparently reduced persistence lengths in force-extension relations. We obtain force-extension relations for strong- and weak-stretching regimes which include the effects of extensible bonds, discrete chain structure, and finite polymer length. We discuss the associated characteristic force scales and calculate the crossover behaviour of the force-extension curves. Strong stretching is governed by the discrete chain structure and the bond extensibility. The linear response for weak stretching depends on the relative size of the contour length and the persistence length which affects the behaviour of very rigid filaments such as F-actin. The results for the force-extension relations are corroborated by transfer matrix and variational calculations.

PACS. 87.15.-v Biomolecules: structure and physical properties – 87.15.Aa Theory and modeling; computer simulation – 87.15.La Mechanical properties

1 Introduction

The Kratky-Porod or worm-like chain [1–5] describes inextensible polymers with positional fluctuations that are not purely entropic but governed by their bending energy and characterized by their bending modulus κ or the persistence length. The worm-like–chain model has been successfully applied to stretching experiments on the single-molecule level in order to interpret force-extension relations for single polymer chains. Experimental progress in manipulating single polymeric molecules has been rapid over the past decade and stretching experiments have become possible for a number of bio- and synthetic polymers such as DNA [6,7], polysaccharides [8], polyelectrolytes [9], proteins like titin [10,8] and actin filaments [11]. In all of these experiments the force-extension relation obtained by Marko and Siggia in [12] for a worm-like chain has been used to interpret the results. The main characteristic of this relation for an inextensible worm-like chain of contour length L is an end-to-end extension L_f in the direction of the stretching force $\mathbf{f}$ that is saturating as $1 - L_f/L \propto 1/\sqrt{f}$ for large stretching forces $f = |\mathbf{f}|$ [12].

One assumption underlying the original worm-like–chain model is the inextensibility of the polymer chain. This assumption is clearly violated in the limit of a large tensile force when the elasticity of molecular bonds is probed as is also seen in experiments on DNA [13], polyelectrolytes [9] and F-actin [11] where L_f exceeds L and a *linear* force-extension relation $L_f/L - 1 \propto f$ is seen at larger forces as compared to the characteristic $f^{-1/2}$-saturation of the inextensible worm-like chain. In references [3,14–16] the extensibility of the polymer has been accounted for by correcting the overall relative extension L_f/L by an additional term f/k, where k is the stretching modulus of the polymer. In reference [17] microscopic degrees of freedom for stretchable bond lengths have been included into a worm-like–chain model to allow for a systematic statistical-mechanics treatment of the finite extensibility.

In this paper, we introduce a description of extensible semiflexible polymers by a *semiflexible harmonic chain* (SHC) model which incorporates elastic bonds with non-zero equilibrium bond length as microscopic degrees of freedom into a discrete version of the worm-like chain. The SHC model allows us to study effects of bending rigidity, bond extension, discrete chain structure, and finite length of a semiflexible polymer on the force-extension behaviour in a unified manner. We do not include further internal degrees of freedom such as twist as occurs, for example, in DNA where a transition from B-DNA to overstretched S-DNA is observed at very large forces following the linear

[a] e-mail: kierfeld@mpikg-golm.mpg.de

force dependence within the B-DNA regime that we want to address in this work. In calculating the work done by the stretching force we take into account the thermal fluctuations of the variable bond length. The resulting force-extension relations for the SHC can be calculated for large tensile forces by expanding around the stretched configuration, for small forces by an expansion in powers of f, and finally we use transfer matrix methods analogous to reference [12] to obtain force-extension relations applicable also in the intermediate force regime. We find that the coupling between external force and bond extension gives rise to an effectively increased stretching force. If experimental force-extension curves are analyzed using the standard model of an inextensible worm-like chain, this leads to an apparently reduced persistence length. The corrections calculated within this article for the SHC model can be used to extract the actual rather than the apparent bending rigidity or persistence length from experimental force-extension curves. At very large stretching forces the correlation length is decreased below the bond length and we find a different force-extension relation with a f^{-1}-saturation as for a freely jointed chain due to the discrete chain structure [18]. We explicitly calculate the corresponding crossover function for the force-extension relation of the SHC. Furthermore, we calculate finite-size corrections at small forces which are relevant for experiments on biopolymers such as F-actin [11] with contour length comparable to the persistence length. Effects from the extensibility, corrections due to the discrete chain structure, and finite-size corrections can all be included in interpolation formulae for the force-extension curves of the SHC that are accurate within 10%.

2 The semiflexible harmonic chain model

A semiflexible polymer or filament can be modeled by a discrete chain of N bonds of length b_0 with directions described by unit tangent vectors $\mathbf{t}(n)$ with $|\mathbf{t}(n)| = 1$ that are indexed by the integer bond number $n = 1, \ldots, N$, see Figure 1. The contour length of the polymer is $L = Nb_0$. The bonds can represent either actual chemical bonds in a polymer or larger segments of a filament, for example a helical repeat unit in F-actin. The bonds or segments can be tilted against each other and eventually stretched. The bond vectors connect $N + 1$ "particles" indexed by the integer particle number $i = 0, \ldots, N$ at positions $\mathbf{r}(i) = \mathbf{r}(0) + \sum_{n=1}^{i} b_0 \mathbf{t}(n)$, where $\mathbf{r}(0)$ is the position of the particle at the fixed end of the polymer. Throughout the article, we will discuss the general case of d spatial dimensions. Experimentally relevant are the cases $d = 2$, corresponding to semiflexible polymers which adhere to a substrate [19] or are confined in a slab-like geometry, and $d = 3$.

2.1 Discrete model

In order to describe an *extensible* semiflexible chain we introduce harmonic bonds of variable length $b(n)$ with a

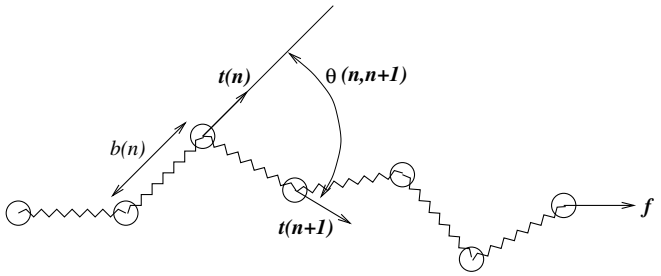

Fig. 1. The semiflexible harmonic chain (SHC) model. $\mathbf{t}(n)$ are bond directions with $|\mathbf{t}(n)| = 1$, $b(n)$ the bond lengths, and $\mathbf{f}$ the external force applied to one end of the polymer. The other end is fixed.

stretching energy

$$E_{\mathrm{s}} = \sum_{n=1}^{N} \frac{k(n)}{2} (b(n) - b_0)^2 = \sum_{n=1}^{N} \frac{k(n) b_0^2}{2} \epsilon^2(n) \,. \qquad (1)$$

Each bond has the equilibrium length b_0 and

$$\epsilon(n) \equiv (b(n) - b_0)/b_0 \qquad (2)$$

are the relative bond extensions. The bonds act as harmonic elastic springs characterized by bond stretching moduli $k(n)$, which we can allow to depend on the bond index n to model spatial heterogeneity.

For an extensible chain the work done by the external force $\mathbf{f}$ applied to one end $\mathbf{r}(N)$ of the chain with the other end $\mathbf{r}(0)$ fixed is

$$E_f = -\mathbf{f} \cdot (\mathbf{r}(N) - \mathbf{r}(0)) = -\sum_{n=1}^{N} b_0 (1 + \epsilon(n)) \mathbf{f} \cdot \mathbf{t}(n) \,. \quad (3)$$

In a semiflexible chain the tilting of neighbouring bonds costs a bending energy [2,4,5]

$$\begin{aligned} E_{\mathrm{b}} &= \sum_{n=1}^{N-1} \frac{\kappa}{2b_0} \left(\mathbf{t}(n+1)) - \mathbf{t}(n)\right)^2 \\ &= \sum_{n=1}^{N-1} \frac{\kappa}{b_0} \left(1 - \cos\theta(n, n+1)\right) \end{aligned} \qquad (4)$$

which only depends on the angles $\theta(n, n+1) = \arccos(\mathbf{t}(n) \cdot \mathbf{t}(n+1))$ enclosed by unit tangent vectors, see Figure 1, and one material parameter, the bending rigidity κ. The bending potential is periodic in the tilt angles $\theta(n, n+1)$ and quadratic for small tilt angles.

The sum of bending and stretching energies (4) and (1) together with the work (3) of the external force gives the Hamiltonian for the discrete *semiflexible harmonic chain* (SHC):

$$\begin{aligned} \mathcal{H}\{\mathbf{t}(n), \epsilon(n)\} &= E_{\mathrm{b}} + E_{\mathrm{s}} + E_f = \\ &\sum_{n=1}^{N-1} \frac{\kappa}{2b_0} \left(\mathbf{t}(n+1)) - \mathbf{t}(n)\right)^2 \\ &+ \sum_{n=1}^{N} \frac{k(n) b_0^2}{2} \epsilon^2(n) - \sum_{n=1}^{N} b_0 (1 + \epsilon(n)) \mathbf{f} \cdot \mathbf{t}(n) \,. \end{aligned} \qquad (5)$$

Note that in the absence of a stretching force $f = 0$ there is no direct coupling between the bond directions $\mathbf{t}(n)$ and the relative bond extensions $\epsilon(n)$. Within the SHC model the bending energy (4) is unaffected by bond stretching or compression and only depends on the angles $\theta(n, n+1)$ between neighbouring bonds and not on their extensions. This aspect of the SHC model is further justified in Appendix A on the basis of elasticity theory of thin elastic rods. In general, a direct coupling between stretching and bending will lead to additional parameters in the model as given by (5).

In the SHC model we use use harmonic bonds as we assume that stretching forces or thermal fluctuations are not sufficient to probe the regime of anharmonic bond stretching potentials [17]. Such anharmonic effects in the bond extensibility have been discussed in reference [17] where synthetic polymers, *i.e.*, alkane chains, have been considered in detail. We expect the characteristic force scales needed to probe such anharmonicities to be comparable to forces that induce structural transitions (such as overstretching of DNA) or even rupture of the semiflexible polymer. As the description of such transitions is outside the scope of the present approach because they require a more microscopic model, we limit ourselves to the regime of harmonic bond potentials.

In reference [20] a discrete model for the stretching of a semiflexible chain has been introduced, which is based on a Gaussian chain model [21]. A continuum version of the Gaussian semiflexible chain has also been studied in reference [22]. In these models the segment lengths are also variable as in the SHC model but they are Gaussian distributed corresponding to zero equilibrium chain length, *i.e.*, $b_0 = 0$. Furthermore, in the Gaussian chain models the bond stretching moduli $k(n)$ are no material parameters but Lagrange multipliers which are adjusted to give prescribed mean extensions $\langle \epsilon(n) \rangle$ appropriate for an inextensible chain. Therefore, as opposed to the extensible SHC model, the Gaussian chains studied in references [22] and [20] are effectively inextensible chains although they involve a calculus with variable bond lengths.

In order to study the force-extension behaviour, discrete models of semiflexible polymers have also been used in references [18] or [23], and bond extension has been taken into account in references [14] and [17]. The SHC model (5) includes a discrete chain structure of finite length with bending energy and extensible bonds within a single model.

In single-molecule stretching experiments two kinds of boundary conditions can be realized. Whereas the positions $\mathbf{r}(0)$ and $\mathbf{r}(N)$ of the particles at the polymer ends are always under experimental control and thus fixed, we can consider clamped ends with fixed tangents $\mathbf{t}(1)$ and $\mathbf{t}(N)$ as in [24] or free ends where $\mathbf{t}(1)$ and $\mathbf{t}(N)$ can fluctuate. In the partition function of the discrete SHC (5) we sum over all tangent configurations $\mathbf{t}(n)$ according to the boundary conditions of clamped or free ends and subject to the local constraint $|\mathbf{t}(n)| = 1$ and also over all possible bond lengths $b(n)$ or relative bond extensions $\epsilon(n)$. In contrast to [24], we focus on single-molecule stretching experiments with *free* ends where *all* bond directions fluctuate and the partition sum is given by

$$Z = \prod_{n=1}^{N} \int \mathrm{d}\mathbf{t}(n) \delta(|\mathbf{t}(n)| - 1) \prod_{n=1}^{N} \int \mathrm{d}\epsilon(n) e^{-\mathcal{H}\{\mathbf{t}(n), \epsilon(n)\}/T} \tag{6}$$

(we absorb the Boltzmann constant k_B in the symbol T). The integrations over bond extensions $\epsilon(n)$ in (6) are Gaussian and can be readily performed to obtain an effective Hamiltonian only depending on the tangent configurations $\mathbf{t}(n)$:

$$\begin{aligned} \mathcal{H}_\mathrm{eff}\{\mathbf{t}(n)\} &= -T \ln \left[\prod_{n=1}^{N} \int \mathrm{d}\epsilon(n) e^{-\mathcal{H}\{\mathbf{t}(n), \epsilon(n)\}/T} \right] \\ &= \sum_{n=1}^{N-1} \frac{\kappa}{2b_0} \left(\mathbf{t}(n+1)) - \mathbf{t}(n) \right)^2 \\ &\quad - \sum_{n=1}^{N} b_0 \mathbf{f} \cdot \mathbf{t}(n) - \sum_{n=1}^{N} \frac{1}{2k(n)} \left(\mathbf{f} \cdot \mathbf{t}(n) \right)^2 \\ &\equiv \mathcal{H}_\mathrm{i}\{\mathbf{t}(n)\} - \sum_{n=1}^{N} \frac{1}{2k(n)} \left(\mathbf{f} \cdot \mathbf{t}(n) \right)^2 . \end{aligned} \tag{7}$$

The last term in (7) stems from the coupling of fluctuating elastic bonds to the external force and is absent for an *inextensible* discrete worm-like chain with Hamiltonian $\mathcal{H}_\mathrm{i}\{\mathbf{t}(n)\}$ that is obtained in the limit of large stretching moduli $k(n)$. Inspecting the signs in (7) shows that this term leads to an effectively increased stretching force.

2.2 Continuum model

In the limit of small bond lengths b_0 we can switch to a continuous description using a parameterization by arc length $s = nb_0$ of the *unstretched* configuration, in which the contour $\mathbf{r}(s)$ of the extensible semiflexible polymer is described by $\mathbf{r}(s) - \mathbf{r}(0) = \int_0^s \mathrm{d}\tilde{s} (b(\tilde{s})/b_0) \mathbf{t}(\tilde{s})$. The continuous version of the SHC Hamiltonian (5) becomes [3]

$$\begin{aligned} \mathcal{H}\{\mathbf{t}(s), \epsilon(s)\} = \int_0^L \mathrm{d}s \Bigg[&\frac{\kappa}{2} (\partial_s \mathbf{t})^2 + \frac{k(s) b_0}{2} \epsilon^2(s) \\ &- (1 + \epsilon(s)) \mathbf{f} \cdot \mathbf{t}(s) \Bigg] \end{aligned} \tag{8}$$

In the inextensible limit of large stretching moduli $k(s)$ fluctuations in the bond length can be neglected ($\epsilon(s) = 0$) and the continuous SHC Hamiltonian (8) reduces to the inextensible worm-like chain Hamiltonian [1,2]

$$\mathcal{H}_\mathrm{i}\{\mathbf{t}(s)\} = \int_0^L \mathrm{d}s \left[\frac{\kappa}{2} (\partial_s \mathbf{t})^2 - \mathbf{f} \cdot \mathbf{t}(s) \right] . \tag{9}$$

In the absence of a stretching force $\mathbf{f} = 0$ the correlation function of the tangent vectors $\mathbf{t}(s)$ of the worm-like chain fall off exponentially [21,25]

$$\langle \mathbf{t}(s) \cdot \mathbf{t}(0) \rangle = \frac{1}{d} \exp(-s/\tilde{L}_\mathrm{p}) , \tag{10}$$

thereby defining a characteristic length scale, the *persistence length* L_p [26]

$$L_\mathrm{p} \equiv (d-1)\tilde{L}_\mathrm{p} \equiv 2\kappa/T \ . \tag{11}$$

As in the discrete SHC model, the Gaussian path integral over bond extensions $\epsilon(s)$ can be performed also for the continuous SHC Hamiltonian (8) to give the effective continuous Hamiltonian

$$\mathcal{H}_\mathrm{eff}\{\mathbf{t}(s)\} = \mathcal{H}_\mathrm{i}\{\mathbf{t}(s)\} - \int_0^L \mathrm{d}s \frac{1}{2k(s)b_0} \left(\mathbf{f}\cdot\mathbf{t}(s)\right)^2 \tag{12}$$

which is the analogon of (7) and has also been derived in [17].

In the following we will employ different approximate methods to obtain force-extension relations for the effective Hamiltonians (7) or (12) describing the SHC. The extension L_f in force direction is always found from the dependence of the free energy $F(f) = -T\ln Z(f)$ on the force $f = |\mathbf{f}|$ by the thermodynamic relation

$$L_f \equiv \left\langle (\mathbf{r}(L) - \mathbf{r}(0)) \cdot \frac{\mathbf{f}}{f} \right\rangle = -\partial_f F(f) \ . \tag{13}$$

3 Force scales

The SHC models as introduced above contain the following dimensionful parameters: the mean bond length b_0 which represents the basic length scale; the contour length of the SHC $L = Nb_0$; the bond stretching modulus $k(n) = k$ which we will take to be position independent in this section and which has the dimension of energy divided by length squared; the bending rigidity κ which has the dimension energy times length; and the temperature T which has the dimension of energy (in the units used here). These parameters define four different force scales

$$\begin{aligned} &f_\mathrm{cr} \equiv T^2/\kappa\,, \qquad f_L \equiv \kappa/L^2\,, \\ &f_\kappa \equiv 4\kappa/b_0^2\,, \qquad \text{and} \quad f_k \equiv kb_0, \end{aligned} \tag{14}$$

that govern the stretching of the SHC.

3.1 Crossover force scale f_{cr}

First we consider the limiting case of an inextensible chain corresponding to the limit of large stretching modulus k ($f \ll f_k$). If one further considers the continuum limit of small segment sizes b_0 effects of the discrete chain structure become irrelevant ($f \ll f_\kappa$). Then we consider the simplest model (9) describing an inextensible worm-like chain. In the thermodynamic limit of an infinite chain ($f_L = 0$) we are left with only two parameters, namely T and κ, which define a single force scale,

$$f_\mathrm{cr} \equiv T^2/\kappa = 2T/L_\mathrm{p} = 4\kappa/L_\mathrm{p}^2 \ . \tag{15}$$

To elucidate the significance of f_cr as a crossover force scale from weak to strong stretching we introduce a "blob" picture of the stretched inextensible worm-like chain.

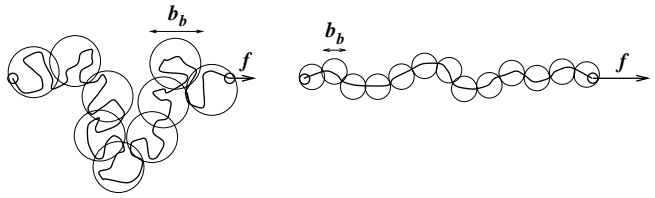

Fig. 2. Left: weak stretching of a semiflexible polymer for $f < f_\mathrm{cr}$ or $\xi_f > L_\mathrm{p}$. Right: strong stretching for $f > f_\mathrm{cr}$ or $\xi_f > L_\mathrm{p}$.

To introduce the characteristic size of a blob we consider an initially straight segment of length ℓ. Bending the segment to an angle $\Delta\theta$ costs an energy $\Delta E_\mathrm{b} \simeq \kappa\Delta\theta^2/\ell$. Additionally, work $\Delta E_f \simeq f\ell\Delta\theta^2$ has to be performed to bend the segment against the external force f. Balancing both energies sets a blob length $\ell = \xi_f$ with

$$\xi_f \simeq \sqrt{\kappa/f} \simeq L_\mathrm{p}\sqrt{f_\mathrm{cr}/f} \ . \tag{16}$$

On small scales $\ell < \xi_f$ inside each blob, we can neglect the external force f and find an unstretched ($f = 0$), thermally fluctuating inextensible SHC. On larger scales $\ell > \xi_f$, we can neglect the bending energy, and the blobs form an effective freely jointed chain of blobs, which is stretched by the external force f and whose bond length b_b is set by the size of a blob, as shown in Figure 2.

Each blob consists of an unstretched inextensible SHC segment of length ξ_f such that the blob size $b_\mathrm{b} = \langle(\mathbf{r}(\xi_f) - \mathbf{r}(0))^2\rangle_0^{1/2}$ is given by the end-to-end distance calculated with respect to the continuum worm-like–chain Hamiltonian (9) in the absence of an external force $f = 0$. Using the correlation function (10) of the tangent vectors $\mathbf{t}(s)$ of a worm-like chain, this leads to a blob size

$$b_\mathrm{b} = \xi_f \mathcal{L}_\mathrm{b}^{1/2}\left(\tilde{L}_\mathrm{p}/\xi_f\right) \approx \begin{cases} (2\xi_f\tilde{L}_\mathrm{p})^{1/2}\,, & \text{for } \xi_f \gg \tilde{L}_\mathrm{p}\,, \\ \xi_f\,, & \text{for } \xi_f \ll \tilde{L}_\mathrm{p}\,, \end{cases} \tag{17}$$

with a scaling function $\mathcal{L}_\mathrm{b}(x) \equiv 2x\left(1 - x + xe^{-1/x}\right)$. For $\xi_f \ll \tilde{L}_\mathrm{p}$ the blobs essentially consist of rigid rods of length $b_\mathrm{b} \approx \xi_f$; for $\xi_f \gg \tilde{L}_\mathrm{p}$ each blob consists of a flexible chain of size $b_\mathrm{b} \propto \xi_f^{1/2}$.

The blobs form an effective freely jointed chain under tension by the external force f. This freely jointed chain of blobs contains L/ξ_f blobs of size b_b. The force-extension relation of a freely jointed chain is well-known for $d = 3$ [27] and discussed in Appendix B for d dimensions. Describing the inextensible SHC as effective freely jointed chain of blobs we expect a force-extension relation that is of the form

$$\frac{L_f}{N_\mathrm{b}b_\mathrm{b}} = \mathcal{F}_d\left[\frac{fb_\mathrm{b}}{T}\right], \tag{18}$$

where $\mathcal{F}_d(x)$ is a scaling function that depends only on the dimensionality d and is similar to the corresponding scaling functions $\mathcal{F}_d^\mathrm{FJC}(x)$ for a freely jointed chain. The effective freely jointed chain shows a characteristic crossover from weak to strong stretching at forces $f \simeq T/b_\mathrm{b}$.

The result (18), together with the relation (17) for the effective bond length, gives the scaling form for the force-extension relation of an inextensible SHC:

$$\frac{L_f}{L} = \frac{b_\mathrm{b}}{\xi_f}\mathcal{F}_d\left[\frac{fb_\mathrm{b}}{T}\right] = \mathcal{G}_d\left[\frac{f}{f_\mathrm{cr}}\right], \qquad (19)$$

where $\mathcal{G}_d(x)$ is another scaling function related to $\mathcal{F}_d(x)$ and $\mathcal{L}_\mathrm{b}(x)$ by

$$\mathcal{G}_d(x^2) = \mathcal{L}_\mathrm{b}^{1/2}(x/(d-1))\mathcal{F}_d\left[2x\mathcal{L}_\mathrm{b}^{1/2}(x/(d-1))\right]. \qquad (20)$$

The scaling form (19) is governed by the force-dependent ratios $L_\mathrm{p}/\xi_f \simeq (f/f_\mathrm{cr})^{1/2}$ and $f\xi_f/T \simeq (f/f_\mathrm{cr})^{1/2}$. Thus, f_cr is the only crossover force scale in the scaling result (19) marking the crossover from weak to strong stretching of the inextensible SHC. At the force scale $f = f_\mathrm{cr}$, the blob size $b_\mathrm{b} \simeq \xi_f \simeq L_\mathrm{p}$ matches both the persistence length L_p and the crossover length ξ_f. The force scale f_cr itself then matches $f_\mathrm{cr} \simeq T/\xi_f \simeq T/b_\mathrm{b}$, and the effective freely jointed chain of blobs undergoes a crossover from weak to strong stretching.

For strong-stretching forces $f \gg f_\mathrm{cr}$ with $\xi_f \ll L_\mathrm{p}$ rigid polymer segments of blob length $b_\mathrm{b} \simeq \xi_f$ form an effective freely jointed chain that is strongly aligned by the stretching force $\mathbf{f}$, see Figure 2. Using the asymptotic behaviour $\mathcal{F}_d(x) \approx 1-(d-1)x/2$ and $\mathcal{L}_\mathrm{b}(x) \approx 1$ for large x, we find the well-known result $1 - L_f/L \simeq \sqrt{f_\mathrm{cr}/f}$ for a worm-like chain close to full stretching [12]. For weak-stretching forces $f \ll f_\mathrm{cr}$ with $\xi_f \gg L_\mathrm{p}$, on the other hand, the blob length ξ_f exceeds the persistence length L_p such that the chain starts to become flexible within each blob. Furthermore, the freely jointed chain of blobs is only weakly aligned, see Figure 2. Using $\mathcal{F}_d(x) \simeq x$ and $\mathcal{L}_\mathrm{b}(x) \simeq x$ for small x we obtain linear-response behaviour $L_f/L \simeq f/f_\mathrm{cr}$ as expected at low tensile forces.

The force scale f_cr is solely determined by the rigidity of the semiflexible polymer. For a rather stiff filament such as F-actin with a persistence length $\tilde{L}_\mathrm{p} \simeq 10\,\mu$m [28] or $L_\mathrm{p} \simeq 20\,\mu$m [26] the crossover force $f_\mathrm{cr} = T^2/\kappa = 2T/L_\mathrm{p}$ between weak and strong stretching is estimated as $f_\mathrm{cr} = 2T/L_\mathrm{p} \sim 4\times10^{-4}$ pN. Such small forces are not experimentally accessible as optical traps or tweezers can be used in order to study forces in the regime of 1pN and magnetic tweezers down to 0.01pN. For less rigid semiflexible biopolymers such as DNA with $L_\mathrm{p} \simeq 100$ nm [29] one finds $f_\mathrm{cr} = 2T/L_\mathrm{p} \sim 8\times10^{-2}$ pN and the force regime of weak stretching is accessible by magnetic tweezers [6].

3.2 Discrete chains and force scale f_κ

The discrete chain structure of the SHC model (7) with a bond length b_0 introduces the force scale

$$f_\kappa \equiv 4\kappa/b_0^2, \qquad (21)$$

where a factor 4 has been included in the definition for later convenience. Effects from the segment size b_0 can be neglected for small forces $f \ll f_\kappa$ or $\xi_f \gg b_0$ where we can use the continuous model (12). For large forces $f \gg f_\kappa$ the crossover length ξ_f becomes smaller than the size b_0 of individual segments of the SHC, and the discrete structure of the SHC becomes relevant. Within the blob scaling picture, the blob length ξ_f has to be replaced then by the segment length b_0 in the scaling result (19) for the force-extension relation.

The force scale f_κ is related to the force scale f_cr by

$$f_\kappa/f_\mathrm{cr} = (L_\mathrm{p}/b_0)^2 \gg 1 \qquad (22)$$

as we will focus on semiflexible polymers, for which the persistence length L_p is large compared to the bond length b_0. Thus, f_κ is always within the strong-stretching regime. $L_\mathrm{p} \gg b_0$ is generally fulfilled for semiflexible biopolymers such as DNA or actin but might be violated for synthetic polyelectrolytes at sufficiently high salt concentration [9]. For typical semiflexible filaments such as F-actin we find $f_\kappa/f_\mathrm{cr} = (L_\mathrm{p}/b_0)^2 \sim 4\times10^6$ with $L_\mathrm{p} \simeq 20\,\mu$m [28] and a segment size $b_0 \simeq 10$ nm [30] that we estimate by the size of a G-actin monomer. This gives rise to large values $f_\kappa \sim 1.6$ nN. For DNA at high salt concentrations one finds values $f_\kappa/f_\mathrm{cr} = (L_\mathrm{p}/b_0)^2 \sim 10^5$ with $L_\mathrm{p} \simeq 100$ nm [29] and a segment size $b_0 \simeq 0.34$ nm set by the distance between base pairs. Accordingly we find an even higher value $f_\kappa \sim 7$ nN.

3.3 Finite chains and force scale f_L

The contour length L of the semiflexible polymer introduces another force scale

$$f_L \equiv \kappa/L^2. \qquad (23)$$

So far we have considered the thermodynamic limit of a long chain such that $f \gg f_L$ or $\xi_f \ll L$ and we can neglect finite-size effects. If $L < \xi_f$, corresponding to small forces $f < f_L$, we expect finite-size effects and a crossover in the force-extension relation. Within the blob picture these finite-size effects can be taken into account by replacing ξ_f by L in the scaling result (19) for the force-extension relation.

The force scale f_L is related to the crossover force scale f_cr by $f_L/f_\mathrm{cr} = L_\mathrm{p}/2L$. For $L > L_\mathrm{p}/2$ or $f_L < f_\mathrm{cr}$ finite-size effects will occur only in the weak-stretching regime for $f < f_L < f_\mathrm{cr}$, whereas for semiflexible polymers with a short contour length, $L < L_\mathrm{p}/2$ or $f_L > f_\mathrm{cr}$, *e.g.* typical actin filaments, finite-size effects will also affect the strong-stretching regime within the force window $f_\mathrm{cr} < f < f_L$.

The force scale f_L is related to the force scale f_κ by

$$f_L/f_\kappa = (b_0/4L)^2 \gg 1 \qquad (24)$$

as the contour length L is always large compared to the segment size b_0, *i.e.*, finite-size effects occuring for $f < f_L$ and effects from the discrete chain structure occuring at $f \gg f_\kappa$ exclude each other.

3.4 Extensibility and force scale f_k

In the SHC model (7) we also allow for extensible segments or bonds with stretching modulus k which introduces the force scale

$$f_k \equiv kb_0 \ . \tag{25}$$

Individual bonds of the discrete SHC as described by (5) have relative extensions $\langle\epsilon\rangle = f/f_k$. Thus they can be considered inextensible for small forces $f \ll f_k$. By definition this force scale also depends on the segment size b_0 which is a consequence of the fact that the introduction of extensible bonds requires a discrete chain structure. Within the model (7), this force scale is independent of the other scales since we can choose an arbitrary value of k. However, we can consider the SHC as a "discretized elastic rod" consisting of circular segments of length b_0 and radius a as is done in Appendix A. For such a model we find $kb_0 \simeq Ea^2$, see (A.2), *i.e.*, the force scale f_k is determined by Young's modulus of the material and the radius a of the rod and thus independent of b_0. This implies that $k \propto b_0^{-1}$ depends on the segment size, and the force scale f_k does not necessarily vanish in the continuum limit of small b_0.

If we consider the SHC as a discretized elastic rod, also the bending rigidity κ and the stretching modulus k are no longer independent but related by elasticity theory according to $kb_0/\kappa \simeq 1/a^2$, see (A.2), and thus

$$f_k/f_\kappa \simeq (b_0/a)^2 \ . \tag{26}$$

This suggests that for long elongated segments with $b_0 \gg a$ we have $f_k \gg f_\kappa$, whereas disc-like segments with $b_0 \ll a$ lead to $f_k \ll f_\kappa$. Experimental values for the force scale f_k have been obtained for F-actin in reference [11] where $f_k \sim 35\,\mathrm{nN}$ is found such that $f_k \gg f_\kappa$.

Using the discretized elastic-rod model we also find

$$f_k/f_{\rm cr} \simeq (L_{\rm p}/a)^2 \gg 1 \quad \text{and} \quad f_k/f_L \simeq (L/a)^2 \gg 1 \tag{27}$$

(which holds regardless of the value of b_0 within the discretized elastic-rod model) as we can assume $L_{\rm p} \gg a$ and $L \gg a$ in general, which is well fulfilled for F-actin with $a \simeq 4\,\mathrm{nm}$ or DNA with $a \simeq 0.8\,\mathrm{nm}$. Therefore, f_k represents a force scale that lies always within the strong-stretching regime. Also, the relative extension of the SHC is insensitive to finite-size effects.

4 Strong stretching $f \gg f_{\rm cr}$

For large stretching forces $f \gg f_{\rm cr}$, the tangent vectors $\mathbf{t}$ deviate only little from the direction set by the force. Therefore we choose our coordinate system such that the direction of the force is the x-direction $\mathbf{f} = f\mathbf{e}_x$ and decompose tangent vectors according to $\mathbf{t} = (t_x, \mathbf{t}_\perp)$ into one component t_x parallel to the force and a $d_\perp = (d-1)$-dimensional vector $\mathbf{t}_\perp$ describing the perpendicular deviations [12]. The local constraint $|\mathbf{t}(n| = 1$ eliminates $t_x(n)$ as a degree of freedom by using $t_x = (1 - \mathbf{t}_\perp^2)^{1/2}$. For strong stretching $\langle t_\perp^2\rangle \ll 1$ is small, and we can expand the effective Hamiltonian (7) of the weakly bent SHC up to second-order terms in $\mathbf{t}_\perp$:

$$\begin{aligned}\mathcal{H}_{\rm eff}\{\mathbf{t}_\perp(n)\} = &\sum_{n=1}^{N-1} \frac{\kappa}{2b_0}(\mathbf{t}_\perp(n) - \mathbf{t}_\perp(n+1))^2 \\ &+ \sum_{n=1}^{N} \frac{fb_0}{2}\left(1 + \frac{f}{k(n)b_0}\right)\mathbf{t}_\perp^2(n) \\ &- Nfb_0 - \sum_{n=1}^{N}\frac{f^2}{2k(n)} \ .\end{aligned} \tag{28}$$

$-Nfb_0$ is the potential energy of the fully stretched chain and the last term in (28) represents the overall elastic energy of the bonds which has been used by Odijk [14] to describe an extensible worm-like chain.

However, we find further effects from extensional fluctuations of elastic bonds that couple both to the external force and the bond directions. Comparing the second term in (28) with the corresponding term in the expansion for the Hamiltonian (9) of the inextensible worm-like chain we read off that corrections due to the coupling of elastic bonds with the external force term lead to an effectively increased force [17]

$$f_{\rm eff}(n) = f\left(1 + \frac{f}{k(n)b_0}\right) = f\left(1 + \frac{f}{f_k}\right) \ , \tag{29}$$

where the last equality holds for homogeneous bonds $k(n) = k$. Note that, for a spatially inhomogeneous, *i.e.*, n-dependent stretching modulus $k(n)$, the effective force and effective bending rigidity become spatially inhomogeneous.

The partition sum of the effective Hamiltonian (28) for free ends is obtained by performing the path integral over the remaining degrees of freedom $\mathbf{t}_\perp(n)$ [31,32]

$$Z(f) = \prod_{n=1}^{N}\int \mathrm{d}\mathbf{t}_\perp(n) e^{-\mathcal{H}_{\rm eff}\{\mathbf{t}_\perp(n)\}/T} \ . \tag{30}$$

For the case of homogeneous bonds $k(n) = k$, this path integral can be directly evaluated. We first perform the path integral for boundary conditions of clamped ends, *i.e.*, with fixed $\mathbf{t}_\perp(1)$ and $\mathbf{t}_\perp(N)$ before we integrate in the end over $\mathbf{t}_\perp(1)$ and $\mathbf{t}_\perp(N)$ to obtain the result for free ends. In order to perform the path integral for clamped ends we consider the "classical path" $\mathbf{t}_\perp^0(n)$ that minimizes the Hamiltonian (28) for boundary conditions $\mathbf{t}_\perp^0(1) = \mathbf{t}_\perp(1)$ and $\mathbf{t}_\perp^0(N) = \mathbf{t}_\perp(N)$ and integrate over fluctuations $\delta\mathbf{t}_\perp(n) = \mathbf{t}_\perp(n) - \mathbf{t}_\perp^0(n)$, which then fulfill boundary conditions $\delta\mathbf{t}_\perp(1) = \delta\mathbf{t}_\perp(N) = 0$ As the Hamiltonian (28) is quadratic, contributions from the classical path $\mathbf{t}_\perp^0(n)$ and fluctuations $\delta\mathbf{t}_\perp(n)$ separate exactly, and

the partition function factorizes into

$$Z(f) = Z_0(f) Z_\delta(f) e^{Lf/T + Lf^2/2Tf_k} , \tag{31}$$

$$Z_0(f) \equiv \left(\prod_{n=1,N} \int \mathrm{d}\mathbf{t}_\perp(n) e^{-\tilde{\mathcal{H}}_{\mathrm{eff}}\{\mathbf{t}^0_\perp(n)\}/T} \right) , \tag{32}$$

$$Z_\delta(f) \equiv \left(\prod_{n=2}^{N-1} \int \mathrm{d}\delta\mathbf{t}_\perp(n) e^{-\tilde{\mathcal{H}}_{\mathrm{eff}}\{\delta\mathbf{t}_\perp(n)\}/T} \right) , \tag{33}$$

where we split off the last two terms of (28) and used $\tilde{\mathcal{H}}_{\mathrm{eff}}\{\mathbf{t}_\perp(n)\} \equiv \mathcal{H}_{\mathrm{eff}}\{\mathbf{t}_\perp(n)\} + Lf + Lf^2/2f_k$. $Z_0(f)$ is the contribution from the integration over the tangents $\mathbf{t}_\perp(1)$ and $\mathbf{t}_\perp(N)$ at the free ends weighted with the energy $\tilde{\mathcal{H}}_{\mathrm{eff}}\{\mathbf{t}^0_\perp(n)\}$ for the classical path, and $Z_\delta(f)$ is the partition function of the fluctuations $\delta\mathbf{t}_\perp(n)$ around the classical path which are weighted with the same Hamiltonian $\tilde{\mathcal{H}}_{\mathrm{eff}}$.

The path integral in the fluctuation contribution $Z_\delta(f)$ can be calculated by using Fourier modes $\delta\mathbf{t}_\perp(n) = \sin(qn)$ with wave vectors $q = m\pi/N$ with $0 < m < N$. For the corresponding contribution $F_\delta(f) = -T \ln Z_\delta(f)$ to the free energy we find

$$\begin{aligned} &\frac{1}{L}\left[F_\delta(f) - F_\delta(0)\right] \approx \\ &\quad d_\perp T \int_0^{\pi/b_0} \frac{\mathrm{d}q}{2\pi} \ln\left(\frac{1-\cos(qb_0) + f_{\mathrm{eff}} b_0^2/2\kappa}{1-\cos(qb_0)} \right) = \\ &\quad \frac{d_\perp T}{b_0} \mathrm{arcsinh}\left[\left(\frac{f_{\mathrm{eff}}}{f_\kappa} \right)^{1/2} \right] , \end{aligned} \tag{34}$$

where we approximated the discrete sum over Fourier modes by an integral as $N \gg 1$.

To calculate the classical path we can use the continuum approximation $x = nb_0$ for small b_0 and find that $\mathbf{t}^0_\perp(x)$ fulfills the equation

$$\partial_x^2 \mathbf{t}^0_\perp = \xi_f^{-2} \mathbf{t}^0_\perp \tag{35}$$

with the crossover length $\xi_f \equiv \sqrt{\kappa/f_{\mathrm{eff}}}$ set by the stretching force, cf. (16). In the limit $L \gg \xi_f$ or $f \gg f_L$ the solution of (35) is approximately $\mathbf{t}^0_\perp(x) \approx \mathbf{t}_\perp(1) e^{-x/\xi_f} + \mathbf{t}_\perp(N) e^{-(L-x)/\xi_f}$, and approaches the straight, force-aligned configuration $\mathbf{t}^0_\perp(x) = 0$ over the characteristic distance ξ_f away from the ends. The corresponding energy is

$$\tilde{\mathcal{H}}_{\mathrm{eff}}\{\mathbf{t}^0_\perp(n)\} \approx \left(\mathbf{t}^2_\perp(1) + \mathbf{t}^2_\perp(N) \right) \frac{1}{2} (\kappa f_{\mathrm{eff}})^{1/2} . \tag{36}$$

Then we can perform the resulting Gaussian integrals in the expression for $Z_0(f)$ to obtain for the corresponding free-energy contribution $F_0(f) = -T \ln Z_0(f)$ in the limit $L \gg \xi_f$ or $f \gg f_L$

$$\frac{1}{L} F_0(f) = \frac{d_\perp T}{2L} \ln\left[4\pi^2 \frac{f_{\mathrm{eff}}}{f_{\mathrm{cr}}} \right] . \tag{37}$$

In the opposite limit $L \ll \xi_f$ or $f \ll f_L$, we can neglect the r.h.s. in (35), and the solution is approximately linear $\mathbf{t}^0_\perp(x) \approx \mathbf{t}_\perp(1) + \frac{x}{L} \Delta\mathbf{t}_\perp$, where $\Delta\mathbf{t}_\perp \equiv \mathbf{t}_\perp(N) - \mathbf{t}_\perp(1)$ with an energy

$$\begin{aligned} \tilde{\mathcal{H}}_{\mathrm{eff}}\{\mathbf{t}^0_\perp(n)\} \approx \frac{\kappa}{2L} \Delta\mathbf{t}^2_\perp + \frac{L f_{\mathrm{eff}}}{2} \\ \times \left(\mathbf{t}^2_\perp(1) - \mathbf{t}_\perp(1) \cdot \Delta\mathbf{t}_\perp + \frac{1}{3} \Delta\mathbf{t}^2_\perp \right) . \end{aligned} \tag{38}$$

Performing the resulting Gaussian integrations in the expression for $Z_0(f)$, we obtain the same result (37) also in the limit $L \ll \xi_f$ or $f \ll f_L$. Together with (34) and the contribution from the remaining factor in (31), we finally obtain the free energy at strong stretching:

$$\begin{aligned} &\frac{1}{L}[F(f) - F(0)] = \\ &\quad -f - \frac{f^2}{2f_k} + 2d_\perp (f_{\mathrm{cr}} f_\kappa)^{1/2} \mathrm{arcsinh}\left[\left(\frac{f_{\mathrm{eff}}}{f_\kappa} \right)^{1/2} \right] \\ &\quad + \frac{d_\perp}{2} (f_{\mathrm{cr}} f_L)^{1/2} \ln\left[\frac{f_{\mathrm{eff}}}{f_{\mathrm{cr}}} \right] , \end{aligned} \tag{39}$$

where we used $T/b_0 = 2(f_{\mathrm{cr}} f_\kappa)^{1/2}$ and $T/L = (f_{\mathrm{cr}} f_L)^{1/2}$. Effects from the extensibility enter this result through the force scale f_k which also occurs in expression (29) for the effective stretching force f_{eff}; effects from the discrete chain structure and the finite chain length enter through the force scales f_κ and f_L, respectively.

Using the thermodynamic relation (13), we arrive at the main result of this section, the force-extension relation for strong stretching:

$$\begin{aligned} \frac{L_f}{L} = \frac{f}{f_k} + 1 \\ - \frac{d_\perp}{4} \left(\frac{f_{\mathrm{cr}}}{f} \right)^{1/2} \frac{1 + 2f/f_k}{(1 + f/f_k)^{1/2}} \frac{1}{(1 + f_{\mathrm{eff}}/f_\kappa)^{1/2}} \\ - \frac{d_\perp}{2} \frac{(f_{\mathrm{cr}} f_L)^{1/2}}{f} \frac{1 + 2f/f_k}{1 + f/f_k} . \end{aligned} \tag{40}$$

This strong-stretching result with its limiting cases will be discussed in detail in Section 6.

The expansion in $\mathbf{t}_\perp$ for a weakly bent SHC is valid as long as $\langle \mathbf{t}^2_\perp \rangle \ll 1$. For the mean-square fluctuations of tangents $\mathbf{t}_\perp(n)$ for the quadratic Hamiltonian (28) we find

$$\begin{aligned} \langle \mathbf{t}^2_\perp \rangle &\approx 2d_\perp \int_0^{\pi/b_0} \frac{\mathrm{d}q}{2\pi} \frac{T}{2\kappa(1-\cos(qb_0))/b_0^2 + f_{\mathrm{eff}}} \\ &= \frac{d_\perp}{2} \left(\frac{f_{\mathrm{cr}}}{f_{\mathrm{eff}}} \right)^{1/2} \frac{1}{(1 + f_{\mathrm{eff}}/f_\kappa)^{1/2}} , \end{aligned} \tag{41}$$

where we approximated the discrete sum over Fourier modes by an integral as $N \gg 1$. Thus, the strong-stretching calculation applies to the force regime $f_{\mathrm{eff}} \gg f_{\mathrm{cr}}$ above the crossover force scale f_{cr}. This confirms the conclusion from the scaling argument in Section 3.1, that f_{cr} is the relevant force scale for the crossover to strong stretching. It also follows that higher-order corrections to (40) will be $\mathcal{O}(f_{\mathrm{cr}}/f_{\mathrm{eff}})$.

5 Weak stretching $f \ll f_{cr}$

For small stretching forces, we can obtain the free energy for the effective Hamiltonian (7) of the SHC by expanding the free energy in the force $\mathbf{f}$ up to second order. In the absence of an external force, the correlation function of the tangent vectors $\mathbf{t}(n)$ can be calculated using angular representations of the Boltzmann weights that have been obtained in the context of path integrals for a quantum particle on the unit sphere in d dimensions in [25]:

$$\langle t_i(n)t_j(n')\rangle_0 = d^{-1}\left(A\left(L_\mathrm{p}/b_0\right)\right)^{|n-n'|}\delta_{ij} \approx \begin{cases} d^{-1}e^{-|n-n'|b_0/\tilde{L}_\mathrm{p}}\delta_{ij}\,, & \text{for } L_\mathrm{p}\gg b_0\,,\\ d^{-1}(L_\mathrm{p}/4b_0)^{|n-n'|}\delta_{ij}\,, & \text{for } L_\mathrm{p}\ll b_0 \end{cases} \tag{42}$$

with a function

$$A(x)\equiv\frac{I_{d/2}(x/2)}{I_{d/2-1}(x/2)}\approx\begin{cases}\exp\left(-(d-1)/x\right)\,, & \text{for } x\gg 1\,,\\ x/4\,, & \text{for } x\ll 1\,,\end{cases} \tag{43}$$

where $I_\nu(x)$ is the Bessel function of order ν [33] and $\tilde{L}_\mathrm{p}$ is defined in (11). The brackets $\langle\ldots\rangle_0$ indicate an expectation value with respect to the SHC Hamiltonian at $f=0$ given by the bending energy (4), $\mathcal{H}_0=E_\mathrm{b}$. In the presence of the external force f, the effective Hamiltonian (7) is divided up according to $\mathcal{H}_\mathrm{eff}=\mathcal{H}_0+\mathcal{H}_f$, and the free energy satisfies the relation $F(f)-F(0)=-T\ln\langle e^{-\mathcal{H}_f/T}\rangle_0$. Performing a cumulant expansion up to second order in $\mathcal{H}_f$ for homogeneous bonds $k(n)=k$ and keeping only terms up to second order in $\mathbf{f}$ leads to

$$\frac{1}{L}\left[F(f)-F(0)\right]\approx-\frac{1}{N}\sum_{n=1}^{N}\frac{1}{2kb_0}\langle(\mathbf{f}\cdot\mathbf{t}(n))^2\rangle_0 -\frac{b_0}{2NT}\sum_{n=1}^{N}\sum_{n'=1}^{N}\langle(\mathbf{f}\cdot\mathbf{t}(n))(\mathbf{f}\cdot\mathbf{t}(n'))\rangle_0. \tag{44}$$

In deriving (44) we used that $\langle\mathbf{f}\cdot\mathbf{t}(n)\rangle_0=0$ as we consider free ends and have to integrate over rotations of $\mathbf{t}(0)$ giving rise to rotations of the entire polymer, in contrast to the situation of clamped ends studied in reference [24]. Both expectation values in the right hand side of this equation involve the correlation function of the tangent vectors $\mathbf{t}$ as given by (42). If the latter expression is inserted, the sums can be performed, and one obtains

$$\frac{1}{L}\left[F(f)-F(0)\right]\approx -\frac{f^2}{2dkb_0}-\frac{f^2b_0}{2dT}\left(\frac{1+A}{1-A}-\frac{2A}{N}\frac{1-A^{N+1}}{(1-A)^2}\right) \tag{45}$$

with $A\equiv A(L_\mathrm{p}/b_0)$.

Focusing on the limit $L_\mathrm{p}\gg b_0$ or $f_\kappa\gg f_\mathrm{cr}$, see (22), we insert the asymptotic expression $A\approx\exp(-b_0/\tilde{L}_\mathrm{p})$, see (43), to obtain

$$\frac{1}{L}\left[F(f)-F(0)\right]\approx-\frac{f^2}{2df_k}-\frac{2}{d(d-1)}\frac{f^2}{f_\mathrm{cr}}\mathcal{L}\left(\frac{\tilde{L}_\mathrm{p}}{L}\right) \tag{46}$$

and the function $\mathcal{L}(x)\equiv\mathcal{L}_\mathrm{b}(x)/2x$ or

$$\mathcal{L}(x)\equiv 1-x+xe^{-1/x}\approx\begin{cases}1-x\,, & \text{for small } x\,,\\ 1/2x\,, & \text{for large } x\,.\end{cases} \tag{47}$$

This function describes finite-size corrections in the free energy which have to be taken into account for polymer contour lengths $L\le\tilde{L}_\mathrm{p}$ comparable or smaller than the persistence length. Using the thermodynamic relation (13), the free energy for weak stretching as given by (46) leads to the force-extension relation

$$\frac{L_f}{L}\approx\left[\frac{1}{df_k}+\frac{4}{d(d-1)}\frac{1}{f_\mathrm{cr}}\mathcal{L}\left(\frac{\tilde{L}_\mathrm{p}}{L}\right)\right]f\,, \tag{48}$$

which is the main result of this section, limiting cases of which will be discussed in Section 6. The extension exhibits a linear-response behaviour as expected for low tensile forces. The first term in (48) represents the effect from the response of the thermally fluctuating extensible bonds and differs by the factor $1/d$ from what has been suggested in reference [15]. The second term represents the contribution from entropic elasticity and bending energy. Relation (48) shows that semiflexible polymers exhibit strong finite-size effects at weak stretching depending on the ratio $\tilde{L}_\mathrm{p}/L=(2/(d-1))(f_L/f_\mathrm{cr})^{1/2}$. As already mentioned the force scale f_κ does not occur in (48) as we work in the continuum limit $f\ll f_\kappa$ assuming that f_κ is inaccessible. Therefore we implicitly assumed $f_k\ll f_\kappa$ in (48).

The cumulant expansion in $\mathcal{H}_f$ for weak stretching is valid for $\langle\mathcal{H}_f^2\rangle_0/T^2\ll 1$ which is equivalent to $f\ll T/\langle(\mathbf{r}(L)-\mathbf{r}(0))^2\rangle_0^{1/2}$ where the mean-square end-to-end distance is obtained as $\langle(\mathbf{r}(L)-\mathbf{r}(0))^2\rangle_0=L\tilde{L}_\mathrm{p}\mathcal{L}(\tilde{L}_\mathrm{p}/L)$. On the other hand, we have argued above that the strong-stretching approximation is valid for $\langle\mathbf{t}_\perp^2\rangle\ll 1$ or $f\gg f_\mathrm{cr}$. In general, these conditions of validity are not complementary, *i.e.*, the weak-coupling expansion is not valid in the entire force range $f\ll f_\mathrm{cr}$ complementary to the strong-stretching force range $f\gg f_\mathrm{cr}$. The reason for this discrepancy is that the external force f can be treated by perturbation theory only for polymer lengths $L<\xi_f$. For larger polymer lengths the integrals over the contour length in (44) will be cut off at the crossover scale ξ_f by non-perturbative corrections. The resulting condition for the validity of the weak-stretching expansion is $f\ll T/\langle(\mathbf{r}(\xi_f)-\mathbf{r}(0))^2\rangle_0^{1/2}$ which is indeed equivalent to $f\ll f_\mathrm{cr}$. This condition is also equivalent to $\xi_f\gg L_\mathrm{p}$ and in this limit our above result (48) is still correct also if L is replaced by ξ_f.

For vanishing κ, the SHC model (7) reduces to an extensible freely jointed chain. This limit corresponds to $L_\mathrm{p}\ll b_0$ or $A\ll 1$ according to (43). The relation (45) then gives

$$\frac{1}{L}\left[F(f)-F(0)\right]\approx-\frac{f^2}{2dkb_0}-\frac{f^2b_0}{2dT} \tag{49}$$

and, using the thermodynamic relation (13), we obtain the force-extension relation of a weakly stretched extensible

freely jointed chain

$$\frac{L_f}{L} \approx \left[\frac{1}{df_k} + \frac{b_0}{dT}\right] f \ . \tag{50}$$

6 Discussion and limiting cases

In this section we will discuss our main results, the force-extension relations (40) for strong stretching $f \gg f_{\rm cr}$ and (48) for weak stretching $f \ll f_{\rm cr}$, and consider various limiting cases along with finite-size effects. These results can also be used to obtain useful interpolation formulae for the whole force range which are derived in Appendix C.

6.1 Extensibility crossover force $f_{k,cr}$

The force-extension relation (40) for strong stretching includes various effects from the bond extensibility of the SHC model (7). Individual bonds of the discrete SHC have relative extensions $\langle\epsilon\rangle = f/f_k$ which give rise to the first term in (40). In the force regime $f \gg f_k$ they are the leading contribution to L_f/L and the SHC is clearly extensible.

In the regime $f \ll f_k$ individual bonds can be considered inextensible, and the first term can be neglected against the second term in (40), which represents the extension of the fully stretched inextensible chain, $L_f/L = 1$. However, as opposed to the extension of individual bonds, the extension of the entire SHC is also governed by much smaller entropic contributions, which give rise to the last two terms in (40). Therefore, the extensibility of the SHC can become already relevant if the bond extension contribution f/f_k exceeds the entropic terms in (40). This happens for forces $f_{k,\rm cr} \ll f \ll f_k$ where the new force scale $f_{k,\rm cr}$ is defined by the condition $L_f/L = 1$ in (40). The force scale $f_{k,\rm cr}$ describes the crossover from an inextensible to an extensible chain within the regime $f \ll f_k$.

Depending on the bond stiffness and thus f_k three different situations (a)-c)) are possible. a) For $f_L \ll f_{k,\rm cr} \ll f_\kappa$ (note that $f_L \ll f_\kappa$, see (24)), effects from the discrete chain structure and finite-size effects can be neglected, and we find [14]

$$f_{k,\rm cr} = \left(\frac{d_\perp}{4}\right)^{2/3} \left(f_k^2 f_{\rm cr}\right)^{1/3}, \quad \text{for } f_L \ll f_{k,\rm cr} \ll f_\kappa \ . \tag{51}$$

As we want to consider the situation $f_{\rm cr} \ll f_k$, see (27), this force scale is indeed much smaller than f_k, *i.e.*, $f_{k,\rm cr} \ll f_k$. b) If the bond stiffness is increased such that $f_L \ll f_\kappa \ll f_{k,\rm cr}$, the discrete chain structure becomes relevant, and we obtain

$$f_{k,\rm cr} = \left(\frac{d_\perp}{4}\right)^{1/2} \left(f_k^2 f_{\rm cr} f_\kappa\right)^{1/4}, \ \text{for } f_L \ll f_\kappa \ll f_{k,\rm cr} \ll f_k, \tag{52}$$

which is again much smaller than f_k because we consider $f_\kappa \ll f_k$ and $f_{\rm cr} \ll f_k$. c) Finally, for a very small bond stiffness or very short polymers with $f_{k,\rm cr} \ll f_L \ll f_\kappa$, we find

$$f_{k,\rm cr} = \left(\frac{d_\perp}{2}\right)^{1/2} \left(f_k^2 f_{\rm cr} f_L\right)^{1/4} \ , \ \text{for } f_{k,\rm cr} \ll f_L \ . \tag{53}$$

Also this result for $f_{k,\rm cr}$ is much smaller than f_k as $f_L \ll f_k$, see (27), and $f_{\rm cr} \ll f_k$.

The discrete SHC as described by (7) can be considered inextensible only for small forces $f \ll f_{k,\rm cr} \ll f_k$. The continuous model (12) applies to forces $f \ll f_\kappa$, and thus describes an extensible continuous chain for $f_{k,\rm cr} \ll f \ll f_\kappa$ but an inextensible continuous chain for $f \ll f_{k,\rm cr}$ and $f \ll f_\kappa$. For the inextensible continuous chain we can use the simplest model (9) of an inextensible worm-like chain. For very stiff bonds with $f_\kappa \ll f_{k,\rm cr}$ we thus have to use the discrete SHC model if we want to consider effects from the extensibility, *i.e.*, the force range $f \gg f_{k,\rm cr}$ or even $f \gg f_k$.

In logarithmic plots of force-extension curves for the extensible SHC, *i.e.*, plots of $\ln(f/f_{\rm cr})$ as a function of L_f/L, there is a point of inversion around $L_f/L \sim 1$ or $f \sim f_{k,\rm cr}$ within the strong-stretching regime, which signals the onset of extensibility effects.

6.2 Inextensible, continuous SHC (worm-like chain)

In the limit of $f \ll f_{k,\rm cr} \ll f_k$ and $f \ll f_\kappa$ we are left with an inextensible, continuous SHC described by the worm-like–chain model (9). In this limit our result (40) for *strong stretching* $f \gg f_{\rm cr}$ reduces to

$$\frac{L_f}{L} = 1 - \frac{d_\perp}{4}\left(\frac{f_{\rm cr}}{f}\right)^{1/2} - \frac{d_\perp}{2}\frac{(f_{\rm cr} f_L)^{1/2}}{f} \ . \tag{54}$$

For $f \gg f_L$, finite-size effects are irrelevant, the last term can be neglected, and it remains the well-known result of Marko and Siggia [12]

$$\frac{L_f}{L} \approx 1 - \frac{d_\perp}{4}\frac{T}{\sqrt{f\kappa}}, \quad \text{for} \quad f \gg f_L \ . \tag{55}$$

For $f_L > f_{\rm cr}$ or contour lengths small compared to the persistence length $L < L_{\rm p}/2$, however, there are also finite-size effects for strong stretching in the force range $f_{\rm cr} < f < f_L$. For $f \ll f_L$ the last term dominates

$$\frac{L_f}{L} \approx 1 - \frac{d_\perp}{2}\frac{T}{fL}, \quad \text{for} \quad f \ll f_L \ . \tag{56}$$

Then we find a force-extension relation $1 - L_f/L \propto 1/f$ for large f that is reminiscent of force-extension relations of freely jointed chains. The condition $f_{\rm cr} < f < f_L$ is equivalent to $L_{\rm p} > \xi_f > L$. In terms of the blob picture it means that the entire polymer behaves essentially as a rigid rod that is contained in a single blob. Therefore the force effectively stretches a *single* bond of length L leading to the result (56).

For *weak stretching* $f \ll f_{\rm cr}$ we find from (48) a linear-response behaviour:

$$\frac{L_f}{L} \approx \frac{4}{d(d-1)} \mathcal{L}\left(\frac{\tilde{L}_{\rm p}}{L}\right) \frac{f}{f_{\rm cr}} \,, \tag{57}$$

which has also pronounced finite size effects as described by the function $\mathcal{L}(x)$ (47) and depending on the ratio $\tilde{L}_{\rm p}/L = (2/(d-1))(f_L/f_{\rm cr})^{1/2}$. This might explain difficulties in fitting experimental results for actin filaments [11], which typically have contour lengths comparable to or smaller than the persistence length $L_{\rm p}$. The asymptotic behaviour of $\mathcal{L}(x)$ for small and large x then implies

$$\frac{L_f}{L} \approx \frac{4}{d(d-1)} \frac{f}{f_{\rm cr}} \,, \quad \text{for} \quad L \gg L_{\rm p} \tag{58}$$

and

$$\frac{L_f}{L} \approx \frac{1}{d} \frac{f}{(f_{\rm cr} f_L)^{1/2}} \,, \quad \text{for} \quad L \ll L_{\rm p} \,. \tag{59}$$

6.3 Inextensible SHC

Next we take into account effects from the discrete structure of the SHC, *i.e.*, the force scale f_κ becomes accessible but we still consider an inextensible chain with $f \ll f_{k,\rm cr} \ll f_k$. In particular this implies $f_\kappa \ll f_{k,\rm cr}$ and thus $f_{k,\rm cr}$ is given by (52). Then we can use the SHC model (7) without the last term. For *strong stretching* $f \gg f_{\rm cr}$ the result (40) gives additional corrections leading to

$$\frac{L_f}{L} = 1 - \frac{d_\perp}{4} \left(\frac{f_{\rm cr}}{f}\right)^{1/2} \frac{1}{(1+f/f_\kappa)^{1/2}} - \frac{d_\perp}{2} \frac{(f_{\rm cr} f_L)^{1/2}}{f} . \tag{60}$$

In the limit $f \ll f_\kappa$ the result reduces to the above formula (54) for the inextensible, continuous SHC but for $f \gg f_\kappa$ the behaviour changes, and we find

$$\frac{L_f}{L} = 1 - \frac{d_\perp}{4} \frac{(f_{\rm cr} f_\kappa)^{1/2}}{f} = 1 - \frac{d_\perp}{2} \frac{T}{f b_0} \quad \text{for} \quad f \gg f_\kappa \,, \tag{61}$$

where we can neglect finite-size effects as $f \gg f_\kappa$ entails $f \gg f_L$ according to (24). Thus, we obtain $1 - L_f/L \propto 1/f$ for large f which is reminiscent of force-extension relations for freely jointed-chain models. The limit $f \gg f_\kappa$ can be realized for small bending rigidities κ. For vanishing κ, it is obvious that the inextensible SHC model (7) without the last term indeed reduces to a freely jointed chain. Note that (61) is identical to the strong-stretching limit of the corresponding force-extension relation (B.3) for a freely jointed chain as derived in Appendix B. In terms of the blob picture, this is due to the fact that for $f \gg f_\kappa$ the crossover or blob length becomes smaller than the bond length $\xi_f \ll b_0$ such that the force effectively stretches *independent* discrete bonds as in a freely jointed-chain model [18].

As effects from the discrete chain structure are only relevant for $f \gg f_\kappa$, but we consider the situation $L_{\rm p} \gg b_0$ or $f_\kappa \gg f_{\rm cr}$, see (22), the *weak-stretching* regime $f \ll f_{\rm cr}$ displays the same behaviour as for the inextensible, continuous SHC that we discussed in the previous section. If we allow for $f_\kappa \ll f_{\rm cr}$ or $b_0 \gg L_{\rm p}$, on the other hand, we obtain the freely jointed-chain result (50) for weak stretching $f_\kappa \ll f \ll f_{\rm cr}$.

6.4 Extensible SHC

Now we want to consider the situation where the extensibility of the SHC becomes relevant, *i.e.*, the force range $f \gg f_{k,\rm cr}$ or even $f \gg f_k$. Then we use the full Hamiltonian (7) of the extensible SHC. For *strong stretching* $f_{\rm eff} \gg f_{\rm cr}$ (or $f \gg f_{\rm cr}$ if $f_k \gg f_{\rm cr}$, see (27), holds), we then have to use the full result (40) for the force-extension relation as well. The full result (40) has various limits depending on the relative size of f_κ, f_k, and the stretching force f or $f_{\rm eff}$. They all have in common that for $f_{k,\rm cr} \ll f \ll f_k$ the elastic response of the stretched bonds can no longer be neglected and for $f \gg f_k$ it becomes the leading term, $L_f/L \simeq f/f_k$. The subleading terms can display different behaviour.

In the previous section we have already discussed the inextensible limit of a discrete chain in the force regime $f_\kappa \ll f \ll f_{k,\rm cr}$, where we found a crossover to a freely jointed-chain behaviour resulting in (61). If the chain is extensible and f/f_k is no longer a small parameter, a freely jointed-chain behaviour sets in already for $f_{\rm eff} \gg f_\kappa$, which is equivalent to $f \gg (f_\kappa f_k)^{1/2}$ if $f \gg f_k$, and relation (61) is modified to

$$\frac{L_f}{L} = \frac{f}{f_k} + 1 - \frac{d_\perp}{4} \frac{(f_{\rm cr} f_\kappa)^{1/2}}{f} \frac{1+2f/f_k}{1+f/f_k} \,, \text{ for } f_{\rm eff} \gg f_\kappa \,. \tag{62}$$

The subleading terms $f/f_k + 1 - L_f/L \propto 1/f$ still show force-extension behaviour reminiscent of freely jointed-chain models but with a modified prefactor. The modification of the prefactor leads to an apparently reduced bond length

$$b_{\rm app} = b_0 \frac{1+f/f_k}{1+2f/f_k} \approx b_0 \left(1 - \frac{f}{f_k}\right) \tag{63}$$

of the freely jointed chain as compared to the inextensible case. The force-extension curve as described by (62) has a point of inversion if plotted logarithmically, *i.e.*, $\ln(f/f_{\rm cr})$ as a function of L_f/L. The point of inversion is located at a force $f \approx f_{k,\rm cr}$, where $f_{k,\rm cr}$ is given by (52) in this force regime.

Also in the *weak-stretching* regime $f \ll f_{\rm cr}$ we have to use the full result (48) for an extensible SHC. However, the differences to the results for inextensible chains are small if $f_{\rm cr} \ll f_k$, see (27), as for weak stretching we consider forces $f \ll f_{\rm cr}$ and thus $f \ll f_k$. If we allow for $f_\kappa \ll f_{\rm cr}$ or $b_0 \gg L_{\rm p}$, we obtain the result (50) for a weakly stretched extensible freely jointed chain in the range $f_\kappa \ll f \ll f_{\rm cr}$.

6.5 Extensible, continuous SHC

Finally, we want to consider the extensible, continuous limit of the SHC. This means we consider forces $f_{\rm eff} \ll f_\kappa$ but $f/f_{k,\rm cr}$ or even f/f_k are no longer small. Then we can use the continuous SHC model (12). In particular, we will consider the situation $f \gg f_{k,\rm cr}$, otherwise the chain becomes effectively inextensible again, and our above results for the worm-like chain apply. For *strong stretching* $f_{\rm eff} \gg f_{\rm cr}$ (or $f \gg f_{\rm cr}$ if $f_k \gg f_{\rm cr}$, see (27), holds), our result (40) becomes

$$\frac{L_f}{L} = \frac{f}{f_k} + 1 - \frac{d_\perp}{4}\left(\frac{f_{\rm cr}}{f}\right)^{1/2} \frac{1+2f/f_k}{(1+f/f_k)^{1/2}}\,, \quad \text{for } f \gg f_{k,\rm cr}, f_L\,, \qquad (64)$$

where we have also neglected finite-size corrections as we want to focus on forces $f \gg f_L$. This limiting case has also been obtained in reference [17] and has to be compared to the force-extension relation (55) of Marko and Siggia [12] for the worm-like chain. The first term in (64) is equivalent to the correction introduced already by Odijk [14] and describes the overall elastic response of a chain with stretch modulus k. However, there is an additional correction due to the extensibility in the third term, which gives an apparently reduced bending rigidity

$$\kappa_{\rm app} = \kappa \frac{1+f/f_k}{(1+2f/f_k)^2} \approx \kappa\left(1 - \frac{3f}{f_k}\right) \qquad (65)$$

as compared to the inextensible worm-like chain. The apparent reduction of κ stems from the coupling of thermally fluctuating bond extensions to both the external force and the bond directions. Fits of experimental force-extension curves using the inextensible worm-like–chain model result (55) will thus measure the apparent parameter $\kappa_{\rm app}$ rather than the actual parameter κ.

Only in the force range $f_{k,\rm cr} \ll f \ll f_k$, we can neglect the correction terms such that $\kappa_{\rm app} \approx \kappa$ and we find the force-extension relation proposed by Odijk [14]

$$\frac{L_f}{L} = \frac{f}{f_k} + 1 - \frac{d_\perp}{4}\left(\frac{f_{\rm cr}}{f}\right)^{1/2}, \text{ for } f_k \gg f \gg f_{k,\rm cr}, f_L. \qquad (66)$$

In the absence of finite-size effects, *i.e.*, focusing on forces $f \gg f_L$, the force-extension curves as described by (64) or (66) have a point of inversion if plotted logarithmically, *i.e.*, $\ln(f/f_{\rm cr})$ as a function of L_f/L. The point of inversion is located at a force $f \approx 4^{-2/3} f_{k,\rm cr}$ [14], where $f_{k,\rm cr}$ is given by (51) and $f_{k,\rm cr} \ll f_k$.

6.6 Application: F-actin

In Appendix C, we derive interpolation formulae which interpolate between the weak-stretching and strong-stretching results and are demonstrated to be accurate within 10%. The interpolation formulae can be used to illustrate and apply our results to F-actin (see Fig. 3) whose force-extension relation has been experimentally studied in [11] in $d = 3$.

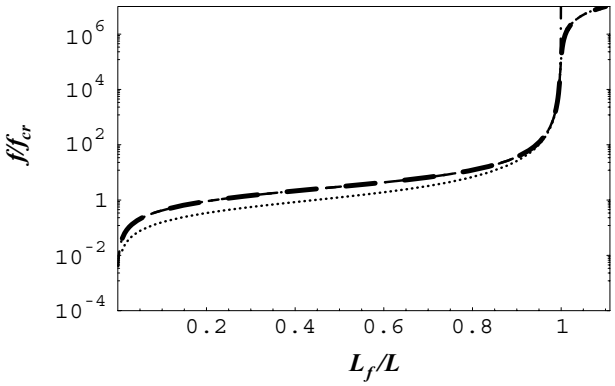

Fig. 3. Logarithmic plots of the force-extension relations ($f/f_{\rm cr}$ as a function of L_f/L) for SHCs in $d = 3$. The thick dashed curve shows the interpolation formulae (C.7) for an *extensible* SHC with parameters $B = 10^{-6}$, $\tilde{L}_{\rm p}/L = 1$, and $f_k/f_{\rm cr} = 10^8$ appropriate for F-actin. The dashed and dotted curves show the limiting cases $B = 0$, $\tilde{L}_{\rm p}/L = 1$ as described by (C.8) and $B = \tilde{L}_{\rm p}/L = 0$ as described by (C.9), respectively. The dash-dotted curve shows an *inextensible* SHC ($f/f_k = 0$) according to (C.4) for the same parameters $B = 10^{-6}$, $\tilde{L}_{\rm p}/L = 1$.

With a measured persistence length $L_{\rm p} \simeq 20\,\mu$m [11, 26], the crossover force $f_{\rm cr} = 2T/L_{\rm p}$ between weak and strong stretching is estimated as $f_{\rm cr} = 2T/L_{\rm p} \sim 4 \times 10^{-5}$ pN for F-actin. In the experiments in [11] stretching was performed with forces up to $f \sim 300$ pN, corresponding to $f/f_{\rm cr} \sim 10^6$. The bond length b_0 for actin can be estimated by the size of a G-actin monomer as $b_0 \simeq 10$ nm [30] such that $b_0/L_{\rm p} \sim 10^{-3}$ or $f_\kappa/f_{\rm cr} \sim 10^6$. For the characteristic stretching force $f_k = kb_0$ a value $f_k \sim 35$ nN has been obtained in reference [11] corresponding to $f_k/f_{\rm cr} \sim 10^8$. This leads to an extensibility crossover force scale $f_{k,\rm cr} \simeq (f_k^2 f_{\rm cr})^{1/3} \sim 40$ pN or $f_{k,\rm cr}/f_{\rm cr} \sim 10^5$, which determines the point of inversion in the logarithmic plots in Figure 3 at $f \approx 4^{-2/3} f_{k,\rm cr}$. In reference [11] the persistence length of F-actin is comparable to the contour length, $L \sim \tilde{L}_{\rm p}$. This leads to rather large corrections at low forces with $\mathcal{L}(\tilde{L}_{\rm p}/L) \approx 0.4$. For $L \sim \tilde{L}_{\rm p}$, the force scale f_L is comparable to $f_{\rm cr}$, *i.e.*, $f_L \sim f_{\rm cr}$.

In Figure 3 we visualize the effects from extensibility, discrete chain structure, and finite-size effects. We show the full interpolation formula (C.7) that includes all three effects in comparison to limiting cases that neglect one of these effects. It is clearly seen that for F-actin finite-size effects have a more pronounced effect on the force-extension curve than effects from the discrete chain structure. Also effects from the extensibility are noticeable at the highest forces [11]. In particular, the point of inversion is well observable in the experiment, although the relative bond extensions are rather small with $\langle\epsilon\rangle = f/f_k \sim 10^{-2}$ for high stretching forces $f \sim 300$ pN.

7 Transfer matrix

The partition sum for the effective continuum Hamiltonian (12) of the extensible SHC can be treated also by the transfer matrix method, which maps the calculation of the partition sum to the diagonalization of a corresponding Hamiltonian operator. On the one hand, we can treat the Hamiltonian operator analytically by an approximate variational calculation to obtain approximate force-extension relations that are more accurate than the interpolation formulae. On the other hand, we can use the transfer matrix method to calculate the exact force-extension curves numerically by diagonalizing the Hamiltonian operator. This also allows to determine the accuracy of the approximate interpolation formulae obtained in Appendix C and the variational calculation.

In the transfer matrix approach we consider first the *restricted* partition sum $Z(\mathbf{t},\mathbf{t}_0;L)$ of the extensible SHC. In the restricted partition sum we apply boundary conditions of clamped polymer ends $\mathbf{t}(0)=\mathbf{t}_0$ and $\mathbf{t}(L)=\mathbf{t}$, and we can write

$$Z(\mathbf{t},\mathbf{t}_0;L)=\int_{(\mathbf{t}_0;0)}^{(\mathbf{t};L)}\mathcal{D}\mathbf{t}(s)\delta(|\mathbf{t}(s)|-1)e^{-\mathcal{H}_{\rm eff}\{\mathbf{t}(s)\}/T} \quad (67)$$

with the effective Hamiltonian (12) after integrating over bond extensions $\epsilon(s)$. It is advantageous to include a constant factor such that the unrestricted partition sum of the unstretched ($f=0$) chain is set to unity which is equivalent to shifting the energy scale such that the free energy of the unrestricted, unstretched chain is set to zero. As a function of the final tangent $\mathbf{t}$ and the polymer length L, the restricted partition sum $Z(\mathbf{t},\mathbf{t}_0;L)$ of the extensible SHC fulfills a Schrödinger-like differential transfer matrix equation [12] in the continuum limit $b_0\to 0$:

$$\partial_L Z(\mathbf{t},\mathbf{t}_0;L)= \left[\frac{T\mathbf{L}^2}{2\kappa}+\frac{\mathbf{f}\cdot\mathbf{t}}{T}+\frac{1}{2k(L)b_0T}\left(\mathbf{f}\cdot\mathbf{t}(s)\right)^2\right]Z(\mathbf{t},\mathbf{t}_0;L)\,, \quad (68)$$

where $\hat{\mathbf{L}}\equiv\mathbf{t}\times\nabla_{\mathbf{t}}$ is the angular-momentum operator. The solution satisfies a boundary condition $Z(\mathbf{t},\mathbf{t}_0;0)=\delta(\mathbf{t}-\mathbf{t}_0)$. To solve (68) for homogeneous bonds $k(s)=k$ we make an Ansatz $Z(\mathbf{t},\mathbf{t}_0;L)=\psi_E(\mathbf{t})\exp(-EL/T)$, where the energy eigenfunction $\psi_E(\mathbf{t})$ for the energy level E fulfills the stationary version of the Schrödinger-like differential transfer matrix equation

$$-E\psi_E(\mathbf{t})=\left[\frac{\hat{\mathbf{L}}^2}{2f_{\rm cr}}+(\mathbf{f}\cdot\mathbf{t})+\frac{1}{2f_k}\left(\mathbf{f}\cdot\mathbf{t}(s)\right)^2\right]\psi_E(\mathbf{t}) \equiv -\hat{H}\psi_E(\mathbf{t})\,, \quad (69)$$

where $\hat{H}$ is the "Hamiltonian" operator of the corresponding quantum problem. The solution satisfying the boundary condition $Z(\mathbf{t},\mathbf{t}_0;0)=\delta(\mathbf{t}-\mathbf{t}_0)$ is obtained by summing over all energy levels E_n

$$Z(\mathbf{t},\mathbf{t}_0;L)=\sum_n\psi_{E_n}(\mathbf{t})\psi_{E_n}(\mathbf{t}_0)e^{-E_nL/T} \approx\psi_{E_0}(\mathbf{t})\psi_{E_0}(\mathbf{t}_0)e^{-E_0L/T}\,, \quad (70)$$

where the ground-state E_0 dominates in the thermodynamic limit $L\gg T/|E_0-E_1|$. In order to study finite-size effects we have to include sufficiently many terms of the sum over eigenstates in (70).

The result (70) applies to clamped boundary conditions. In order to switch to the free boundary conditions that we have used in the previous sections, we integrate over all configurations of initial and final unit tangents and obtain for the partition sum of a SHC of length L

$$Z(L)\approx\left(\int\mathrm{d}\mathbf{t}\psi_{E_0}(\mathbf{t})\right)^2e^{-E_0L/T}\,, \quad (71)$$

where the last line holds in the thermodynamic limit $L\gg T/|E_0-E_1|$, where the ground-state E_0 dominates. In the thermodynamic limit the ground-state energy E_0 determines the free energy

$$\frac{1}{L}\left[F(f)-F(0)\right]=E_0 \quad (72)$$

of the stretched semiflexible polymer. Note that in the thermodynamic limit effects from the boundary conditions can be neglected and equation (72) holds both for free and clamped boundary conditions. This changes for a finite system where we have to keep sufficiently many terms in the sums over eigenstates and find

$$\frac{1}{L}\left[F(f)-F(0)\right]=-\frac{T}{L}\ln\left[\sum_n\psi_{E_n}(\mathbf{t})\psi_{E_n}(\mathbf{t}_0)e^{-E_nL/T}\right] \quad (73)$$

for clamped boundary conditions and

$$\frac{1}{L}\left[F(f)-F(0)\right]=-\frac{T}{L}\ln\left[\sum_n\left(\int\mathrm{d}\mathbf{t}\psi_{E_n}(\mathbf{t})\right)^2e^{-E_nL/T}\right] \quad (74)$$

for free boundary conditions. The extension as a function of the stretching force f can be found by differentiation of the free energies with respect to f using the thermodynamic relation (13).

8 Variational calculation

In this section we study effects of the coupling between external force and extensible bonds for the continuous model of an extensible SHC in the thermodynamic limit by employing the transfer matrix treatment combined with a variational calculation analogous to reference [12]. We reproduce our results for strong and weak stretching but the variational treatment allows to obtain the crossover between the two regimes more accurately than the interpolation formulae presented in Appendix C, also in the presence of the correction term in the effective Hamiltonian (12).

In order to obtain the ground-state energy E_0 of the Schrödinger-like differential transfer matrix equation (69) we apply a variational principle using an Ansatz

$$\psi_a(\mathbf{t})\propto\exp\left(\frac{a}{2}(\mathbf{f}\cdot\mathbf{t})\right) \quad (75)$$

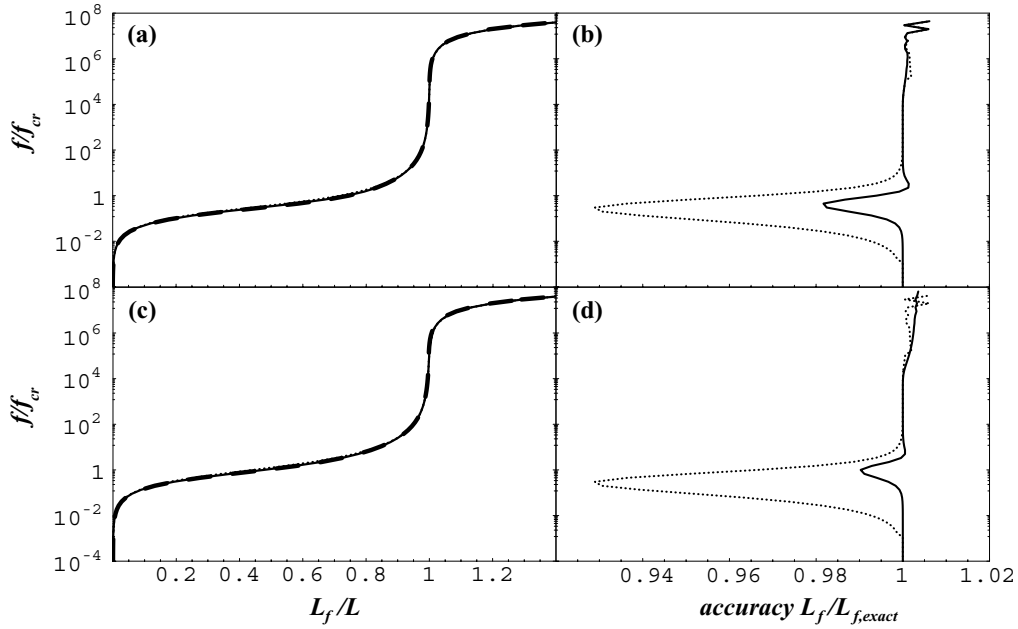

Fig. 4. (a), (c): Force-extension curves ($f/f_{\rm cr}$ as a function of L_f/L) for an extensible, infinite, and continuous SHC ($f_k = 10^8 f_{\rm cr}$, $\tilde{L}_{\rm p}/L = 0$, and $b_0 = 0$) in (a) $d = 2$ and (c) $d = 3$ according to the variational calculation (solid line) and the interpolation formula (C.9) (dotted line) in comparison with the exact numerical force-extension curve (thick dashed line). (b), (d): Force $f/f_{\rm cr}$ *versus* the ratios $L_{f,\rm var}/L_{f,\rm exact}$ (solid line) and $L_{f,\rm inter}/L_{f,\rm exact}$ (dotted line) of the extensions $L_{f,\rm var}$ according to the variational calculation and $L_{f,\rm inter}$ according to the interpolation formula (C.9) and the exact numerical extension $L_{f,\rm exact}$ for (b) $d = 2$ and (d) $d = 3$.

with a variational parameter a [12]. Minimization of the expectation value of the operator $\hat{H}$ with respect to a gives the variational result for the ground-state energy

$$E_0 = \min_a \left\{ \frac{\langle\psi_a|\hat{H}\psi_a\rangle}{\langle\psi_a|\psi_a\rangle} \right\} = \min_a \left\{ \frac{1}{I(af)} \left[\frac{1}{2f_{\rm cr}} \left(\frac{1}{4}(af)^2 (I''(af) - I(af)) + \frac{d-1}{2} af I'(af) \right) - f I'(af) - \frac{f^2}{2f_k} I''(af) \right] \right\}. \quad (76)$$

The scalar product is defined as $\langle f|g\rangle \equiv \int_{S^{d-1}} {\rm d}^{d-1}\mathbf{t} f(\mathbf{t}) g(\mathbf{t})$, where S^{d-1} is the surface of the d-dimensional unit sphere, and we calculated the r.h.s. in terms of the integral $I(af) \equiv \langle\psi_a|\psi_a\rangle$. The force-extension relation is obtained using (13) which gives

$$\frac{L_f}{L} = -\partial_f E_0(f)\,. \quad (77)$$

We will perform the variational calculation both for $d = 2$ and $d = 3$ corresponding to the most important experimental situations of a semiflexible polymer adhered to a substrate or freely suspended in three spatial dimensions. We compare the results from the variational approach with exact numerical diagonalization studies of the Hamiltonian operator $\hat{H}$.

In $d = 2$ we have $I(af) = \langle\psi_a|\psi_a\rangle = 2\pi I_0(af)$ with the Bessel function $I_0(x)$ [33]. Using this in (76) we find the variational free energy

$$E_0 = \min_a \left\{ \frac{I_1(af)}{I_0(af)} \left(\frac{1}{8f_{\rm cr}} af - f + \frac{f^2}{2f_k} \frac{1}{af} \right) - \frac{f^2}{2f_k} \right\}. \quad (78)$$

In $d = 3$ we find $I(af) = \langle\psi_a|\psi_a\rangle = 4\pi (af)^{-1} \sinh(af)$ and thus according to (76) the variational free energy

$$E_0 = \min_a \left\{ \left(\coth af - \frac{1}{af} \right) \left(\frac{1}{4f_{\rm cr}} af - f + \frac{f^2}{f_k} \frac{1}{af} \right) - \frac{f^2}{2f_k} \right\}. \quad (79)$$

In the limit of weak stretching we can expand in $af \ll 1$ and the results for E_0 agree to leading order with equation (44) in the thermodynamic limit $L/\tilde{L}_{\rm p} \gg 1$. In the limit of strong stretching $af \gg 1$ the results for E_0 agree with equation (39) in the continuous limit $b_0 \to 0$ or $f_{\rm eff} \ll f_\kappa$ and for an infinite chain $L \to \infty$ or $f_L = 0$. Therefore, we also recover the corresponding force-extension relations (48) for weak and (64) for strong stretching, respectively.

In the intermediate regime we can find the minimum in (78) or (79) by numerical minimization. The resulting force-extension curves are shown in Figure 4 in comparison with the corresponding interpolation formula (C.9), and the exact numerical force-extension curves that we obtain from the numerical diagonalization of the Hamiltonian operator $\hat{H}$ as explained in Section 9. The interpolation formula (C.9) gives an accurate fit within 10%, whereas the variational calculation is accurate within 1% due to the increased accuracy at intermediate forces $f \sim f_{\rm cr}$.

9 Numerical diagonalization

In order to obtain force-extension curves numerically, we first have to diagonalize the Hamiltonian operator $\hat{H}$ from (69) in a suitable representation to find the energy states E_n and wave functions $\psi_{E_n}(\mathbf{t})$. To study the thermodynamic limit it is sufficient to obtain the ground-state energy E_0.

In $d = 2$ we use a representation

$$\psi_E(\mathbf{t}) = \sum_{m=-\infty}^{\infty} \psi_{E,m} e^{im\phi} \tag{80}$$

by Fourier decomposition on the unit sphere with expansion coefficients $\psi_{E,m}$ and where ϕ is the angle between $\mathbf{f}$ and the unit vector $\mathbf{t}$. In this representation the eigenvalue equation (69) becomes

$$\begin{aligned} E\psi_{E,m} = & \\ \sum_{m'=-\infty}^{\infty} \psi_{E,m'} \Bigg[& \frac{1}{2f_{\mathrm{cr}}} m^2 \delta_{mm'} - \frac{f}{2}(\delta_{m,m'+1} + \delta_{m+1,m'}) \\ & - \frac{f^2}{4f_k}\delta_{mm'} - \frac{f^2}{8f_k}(\delta_{m,m'+2} + \delta_{m+2,m'}) \Bigg]. \end{aligned} \tag{81}$$

In $d = 3$ we use a representation

$$\psi_E(\mathbf{t}) = \sum_{l=0}^{\infty} \psi_{E,l} Y_{l0}(\mathbf{t}) \tag{82}$$

by spherical harmonics $Y_{l0}(\mathbf{t})$, where $\psi_{E,l}$ are expansion coefficients and where we have anticipated that the ground state must have axial symmetry such that there are no components $m \neq 0$. Finally, this leads to the matrix eigenvalue equation

$$\begin{aligned} E\psi_{E,l} = \sum_{l'=0}^{\infty} \psi_{E,l'} \Bigg[& \frac{1}{2f_{\mathrm{cr}}} l(l+1)\delta_{l,l'} \\ & - \frac{f}{(2l'+1)^{1/2}(2l+1)^{1/2}} [l\delta_{l,l'+1} + l'\delta_{l,l'-1}] \\ & - \frac{f^2}{2f_k} \frac{2l^2+2l-1}{(2l-1)(2l+3)} \delta_{l,l'} \\ & - \frac{f^2}{2f_k(2l'+1)^{1/2}(2l+1)^{1/2}} \\ & \times \left(\frac{(l'+1)(l'+2)}{2l'+3}\delta_{l,l'+2} + \frac{(l+1)(l+2)}{2l+3}\delta_{l,l'-2} \right) \Bigg]. \end{aligned} \tag{83}$$

The matrix operators on the r.h.s. of (81) and (83) can be numerically diagonalized on any finite-dimensional subspace $|m| < m_{\max}$ in $d = 2$ or $0 \leq l < l_{\max}$ in $d = 3$.

For an *infinite*, continuous SHC we only need to compute numerically the lowest eigenvalue E_0 of the matrix operators for a given force f in order to find the free energy according to (72). Doing so for two forces $f + \Delta f$ and $f - \Delta f$, we can perform a numerical differentiation with respect to f to obtain the force-extension relation according to the thermodynamic relation (13). Choosing $m_{\max}$ or $l_{\max}$ sufficiently large and Δf sufficiently small any desired accuracy can be reached, and we obtain exact numerical force-extension curves. Force-extension curves obtained by this procedure using subspaces $m_{\max} = 30$ in $d = 2$ and $l_{\max} = 30$ in $d = 3$ are shown in Figures 4(a) and (c) in comparison with the corresponding interpolation formula (C.9) for an infinite, continuous SHC and with the corresponding result from the variational calculation.

For a *finite*, continuous SHC with free boundary conditions we compute all energy levels E_n and all corresponding eigenstates $\psi_{E_n,m}$ in $d = 2$ or $\psi_{E_n,l}$ in $d = 3$ by numerical diagonalization of the matrix operators. Then we use (74) to calculate the free energy for a given force f:

$$\frac{1}{L}\left[F(f) - F(0)\right] = -\frac{T}{L} \ln \left[\sum_n \psi_{E_n,0}^2 e^{-E_n L/T} \right]. \tag{84}$$

In (74) we used that the integral $\int \mathrm{d}\mathbf{t} \psi_{E_n}(\mathbf{t})$ gives the projection to the $m = 0$ and $l = 0$ state in $d = 2$ and $d = 3$, respectively. After calculating (84) numerically for two forces $f + \Delta f$ and $f - \Delta f$, we perform the numerical differentiation with respect to f to obtain the force-extension relation according to the thermodynamic relation (13). The exact numerical force-extension curves for a finite, continuous SHC that are shown in Figure 5 in comparison with the corresponding interpolation formula (C.8) have been obtained by this procedure using subspaces $m_{\max} = 30$ in $d = 2$ and $l_{\max} = 30$ in $d = 3$.

10 Conclusion

We have studied the stretching of extensible semiflexible polymers using the discrete extensible SHC model that additionally contains microscopic degrees of freedom describing elastic bonds. The bond stretching depends on the bond direction such that thermal fluctuations of the bonds length lead to an effectively increased stretching of the bond directions. This manifests as an additional forcing term in the effective Hamiltonian (7) that is obtained after performing the partial trace over thermally fluctuating extensions of the elastic bonds. We derived force-extension relations (40) and (48) for the SHC model for strong and weak stretching, respectively, which took into account effects from the extensibility and the discrete chain structure as well as finite-size effects. The result can be used to discuss various important limiting cases. In the limit of strong stretching the discrete chain structure can lead to behaviour reminiscent of a freely jointed chain at very large tensile forces, whereas for weak stretching a continuous description is fully justified. On the other hand, we have to consider finite-size corrections for weak stretching if the contour length becomes comparable to the persistence length as is typically the case for filamentous semiflexible polymers such as F-actin. The results can be

combined into the interpolation formulae (C.4) and (C.7) for the force-extension relations of extensible semiflexible polymers. A complementary transfer matrix treatment of the SHC model allows to analyze the crossover at intermediate forces using a variational calculation. The numerical transfer matrix diagonalization provides exact numerical force-extension curves which we used to determine the accuracy of interpolation formulae and variational calculation. For the interpolation formulae the agreement is within 10% accuracy, even in the presence of finite-size corrections. Our results are relevant to experiments on DNA or F-actin and we have illustrated our results with explicit estimates for F-actin using the experimental results of reference [11].

One of us (O.N.) thanks the Thai Government for support.

Appendix A. Bending and stretching of elastic rods

In this appendix we want to discuss the possibility of a coupling between bending modes and bond extension based on elasticity theory of thin elastic rods [34] which is the basis of the worm-like–chain model and describes many semiflexible polymers and filaments such as DNA (at high salinity such that non-local effects from electrostatic forces can be neglected) and F-actin surprisingly well [30]. Stretching a thin cylindrical elastic rod of radius a and length L by a factor ϵ and simultaneously bending its center line to a curvature radius R induces strains $u_{xx} = (1+\epsilon)(z/R) + \epsilon$ where we chose coordinates such that the rod is oriented along the x-axis and z describes the coordinate perpendicular to the rod and the "neutral plane" that stays undeformed. The origin $z = 0$ is chosen within this neutral plane, *e.g.* in the center of the cylinder. If E is Young's modulus of the polymer material, stresses are $\sigma_{xx} = Eu_{xx}$ and the elastic energy density is $Eu_{xx}^2/2$. Integrating over the spherical cross-section of the rod gives the elastic energy per length

$$\frac{E_{\rm el}}{L} = \frac{EI}{2}(1+\epsilon)^2\frac{1}{R^2} + \frac{EA}{2}\epsilon^2 \qquad \text{(A.1)}$$

with $I = \pi a^4/4$ and $A = \pi a^2$. The bending rigidity and the stretching modulus of the rod are

$$\kappa = EI \simeq Ea^4 \qquad \text{and} \qquad kb_0 = EA \simeq Ea^2 \ . \qquad \text{(A.2)}$$

The coupling between bending and stretching leads to a bending contribution to the elastic energy which is increased by a factor $(1+\epsilon)^2$ in the presence of stretching.

The result (A.1) for an elastic rod can be applied to a semiflexible polymer with a local bond length $b(s)$, where s is the arc length s of the unstretched chain. Stretching gives rise to local bond extensions $\epsilon(s) = (b(s) - b_0)/b_0$ and a local radius of curvature $R(s) = 1/c(s)$, where $c(s)$ is the curvature of the polymer. The elastic energy of the stretched and bent semiflexible polymer with bending rigidity κ and stretching modulus $k(s)$ is thus

$$E_{\rm el} = \int_0^L {\rm d}s \left\{ \frac{\kappa}{2}(1+\epsilon(s))^2 c(s)^2 + \frac{k(s)}{2}\epsilon(s)^2 \right\} . \qquad \text{(A.3)}$$

We want to compare stretched configurations with *identical* bond directions as described by the unit vectors $\mathbf{t}(s)$. Then the polymer contour $\mathbf{r}(s)$ is given by $\mathbf{r}(s) - \mathbf{r}(0) = \int_0^s {\rm d}\tilde{s}(b(\tilde{s})/b_0)\mathbf{t}(\tilde{s})$ and the local curvature $c(s)$ for fixed bond directions $\mathbf{t}(s)$ changes by stretching to

$$c(s) = \frac{b_0}{b(s)}|\partial_s \mathbf{t}(s)| = (1+\epsilon(s))^{-1}|\partial_s \mathbf{t}(s)| \ , \qquad \text{(A.4)}$$

i.e., the curvature is reduced for a locally stretched chain with $\epsilon(s) > 0$. Using this in expression (A.3) for the elastic energy, we obtain

$$E_{\rm el} = \int_0^L {\rm d}s \left\{ \frac{\kappa}{2}(\partial_s \mathbf{t})^2 + \frac{k(s)}{2}\epsilon(s)^2 \right\} \qquad \text{(A.5)}$$

and bending and stretching degrees of freedom *decouple* in the parameterization by bond extensions $\epsilon(s) = (b(s) - b_0)/b_0$ and bond directions $\mathbf{t}(s)$ as described by the unit vectors $\mathbf{t}(s)$.

Appendix B. Force-extension relation for a freely jointed chain

The force-extension relation for a freely jointed chain with N bonds $\mathbf{b}(n)$ of fixed length $|\mathbf{b}(n)| = b$ in d spatial dimensions can be obtained analytically, see, for example, reference [27] for $d = 3$. For a freely jointed chain the only energy is the work done by the external force $\mathbf{f}$ applied to one end of the chain with the other end fixed

$$E_f = -\sum_{n=1}^{N} \mathbf{f}\cdot\mathbf{b}(n) \ . \qquad \text{(B.1)}$$

As for the SHC the extension L_f in force direction is found from the dependence of the free energy $F(f) = -T\ln Z(f)$ on the force $f = |\mathbf{f}|$ by the thermodynamic relation $L_f = -\partial_f F(f)$, see (13). The integration over the N independent bonds can be performed in angular variables with $\theta = \arccos(\hat{\mathbf{f}}\cdot\hat{\mathbf{b}})$ as angle enclosed by a bond vector $\mathbf{b}$ and the force vector $\mathbf{f}$ which gives

$$Z(f) = \left[c(d)\int_0^\pi {\rm d}\theta (\sin\theta)^{d-2} e^{fb\cos\theta/T} \right]^N \qquad \text{(B.2)}$$

with $c(d) \equiv 2\pi^{d/2}/\Gamma(d/2)$ as surface area of the d-dimensional unit sphere. It is evident that after the remaining θ-integration expression (B.2) depends on the force f only through the combination fb/T. Using $F(f) = -T\ln Z(f)$ and $L_f = -\partial_f F(f)$ this leads to force-extension relations of the form

$$\frac{L_f}{Nb} = \mathcal{F}_d^{\rm FJC}\left(\frac{fb}{T}\right), \qquad \text{(B.3)}$$

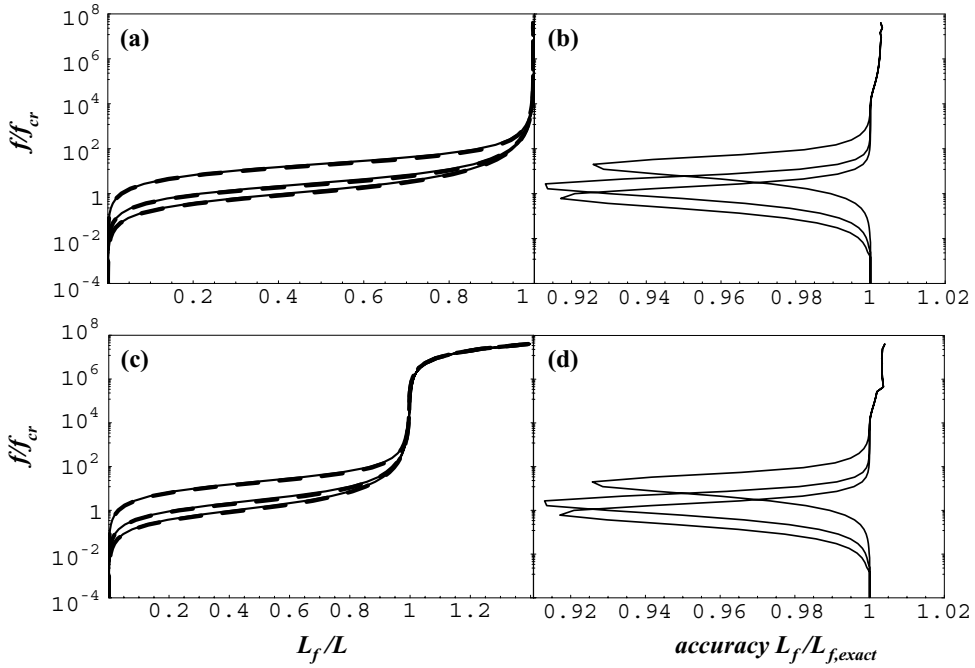

Fig. 5. (a), (c): Force-extension curves ($f/f_{\rm cr}$ as a function of L_f/L) for a continuous ($B = 0$) and (a) inextensible ($f/f_k = 0$) or (c) extensible ($f/f_k = 10^8$) SHC in $d = 3$ according to the interpolation formulae (C.5) and (C.8), respectively (solid lines) and comparison with exact numerical force-extension curves (thick dashed lines) for three different lengths $\tilde{L}_{\rm p}/L = 0.1, 1, 10$ (bottom to top). (b), (d): Force $f/f_{\rm cr}$ *versus* the ratio $L_{f,\rm inter}/L_{f,\rm exact}$ of the extension $L_{f,\rm inter}$ according to the interpolation formulae (C.5) and (C.8), respectively, and the exact numerical extension $L_{f,\rm exact}$ for $\tilde{L}_{\rm p}/L = 0.1, 1, 10$ (bottom to top).

where $\mathcal{F}_d^{\rm FJC}(x)$ is a scaling function that is obtained by explicitly performing the remaining θ-integration and depends only on the dimensionality d.

In $d = 3$ dimensions we find

$$Z(f) = \left[4\pi \sinh\left(\frac{fb}{T}\right)\right]^N . \qquad \text{(B.4)}$$

Using $F(f) = -T \ln Z(f)$ and $L_f = -\partial_f F(f)$ we obtain the result

$$\mathcal{F}_3^{\rm FJC}(x) = 1/\tanh x - 1/x \qquad \text{(B.5)}$$

for the scaling function.

In $d = 2$ dimensions we find

$$Z(f) = \left[2\pi I_0\left(\frac{fb}{T}\right)\right]^N \qquad \text{(B.6)}$$

which leads to the scaling function

$$\mathcal{F}_2^{\rm FJC}(x) = I_1(x)/I_0(x) . \qquad \text{(B.7)}$$

$I_0(x)$ and $I_1(x)$ are Bessel functions [33].

The freely jointed chain shows a crossover from weak to strong stretching for forces $f \simeq T/b$. This is seen in the asymptotics of the scaling function $\mathcal{F}_d^{\rm FJC}(x)$. The scaling function approaches unity or full stretching as $\mathcal{F}_d^{\rm FJC}(x) \approx 1 - (d-1)/2x$ for large x corresponding to large forces $f \gg T/b$, and a linear response $\mathcal{F}_d^{\rm FJC}(x) \approx x/d$ for small x or small forces $f \ll T/b$.

Appendix C. Interpolation formulae

Our force-extension relation (40) for strong stretching $f \gg f_{\rm cr}$ of the SHC, and (48) for weak stretching can be used to obtain interpolation formulae for the whole force range which also account for the corrections due to extensible bonds, discrete chain structure, and finite length of the polymer.

Appendix C.1. Inextensible SHC

For the *inextensible* SHC, we start the construction of interpolation formulae from the strong-stretching result (60) for the inextensible SHC valid for $f \ll f_{k,\rm cr}$. If the last term in (60) containing finite-size corrections is neglected we can solve for the force f and find

$$\frac{f}{f_{\rm cr}} = -\frac{1}{2B} + \frac{1}{2B}\left(1 + \frac{d_\perp^2}{4}\frac{B}{(1-\ell_f)^2}\right)^{1/2} , \qquad \text{(C.1)}$$

where $\ell_f \equiv L_f/L$ is the relative extension and

$$B \equiv f_{\rm cr}/f_\kappa = (b_0/L_{\rm p})^2 \qquad \text{(C.2)}$$

a dimensionless parameter characterizing the discrete chain structure. For $f/f_{\rm cr} \gg 1/B$ or $f \gg f_\kappa$ this formula gives the crossover from the worm-like–chain behaviour $f \propto (1-\ell_f)^{-2}$ for $f \ll f_\kappa$ to the freely jointed-chain behaviour $f \propto (1-\ell_f)^{-1}$ for $f \gg f_\kappa$ due the discrete

chain structure, see (55) and (61). The additional finite-size corrections for strong stretching in (60) can be taken into account to a good approximation by adding another term

$$\frac{f}{f_{\rm cr}} = -\frac{1}{2B} + \frac{1}{2B}\left(1+\frac{d_\perp^2}{4}\frac{B}{(1-\ell_f)^2}\right)^{1/2} + \frac{d_\perp}{4}\frac{L_{\rm p}}{L}\frac{1}{1-\ell_f} \tag{C.3}$$

which gives the correct crossover between the worm-like–chain behaviour $f \propto (1-\ell_f)^2$ for $f \gg f_L$ to the effective rigid-rod result $f \propto (1-\ell_f)$ for $f \ll f_L$, see (55) and (56). Now we add constants and terms linear in ℓ_f to correctly reproduce the linear-response behaviour (48) at weak stretching. This gives the interpolation formula

$$\begin{aligned}\frac{f}{f_{\rm cr}} = \frac{1}{2B}&\left[\left(1+\frac{d_\perp^2}{4}\frac{B}{(1-\ell_f)^2}\right)^{1/2} - \left(1+\frac{d_\perp^2}{4}B\right)^{1/2}\right] \\ &+\frac{d_\perp}{4}\frac{L_{\rm p}}{L}\left(\frac{1}{1-\ell_f}-1\right) \\ &+\left(-\frac{d_\perp^2}{8}\left(1+\frac{d_\perp^2}{4}B\right)^{-1/2} - \frac{d_\perp}{4}\frac{L_{\rm p}}{L}\right. \\ &\left.+\frac{d(d-1)}{4}\frac{1}{\mathcal{L}\big(\tilde{L}_{\rm p}/L\big)}\right)\ell_f\end{aligned} \tag{C.4}$$

with $\tilde{L}_{\rm p} = L_{\rm p}/(d-1)$ and $\mathcal{L}(x)$ as in (47). Finite-size corrections for $L < \tilde{L}_{\rm p}$ at weak stretching are included by the factor $\mathcal{L}(\tilde{L}_{\rm p}/L)$, cf. (48). For $B \ll 1$ effects from the discrete chain structure become negligible and the interpolation formula (C.4) reduces to

$$\begin{aligned}\frac{f}{f_{\rm cr}} = &\frac{d_\perp^2}{16}\left(\frac{1}{(1-\ell_f)^2}-1\right) + \frac{d_\perp}{4}\frac{L_{\rm p}}{L}\left(\frac{1}{1-\ell_f}-1\right) \\ &+\left(-\frac{d_\perp^2}{8} - \frac{d_\perp}{4}\frac{L_{\rm p}}{L} + \frac{d(d-1)}{4}\frac{1}{\mathcal{L}\big(\tilde{L}_{\rm p}/L\big)}\right)\ell_f\,.\end{aligned} \tag{C.5}$$

If we also consider the limit of an infinite chain $L_{\rm p} \ll L$ we obtain

$$\frac{f}{f_{\rm cr}} = \frac{d_\perp^2}{16}\left(\frac{1}{(1-\ell_f)^2}-1\right) + \frac{d^2-1}{8}\ell_f \tag{C.6}$$

which agrees with the well-known interpolation formula of reference [12] for $d = 3$.

The finite-size effects described by (C.4) or (C.5) lead to pronounced corrections in the force-extension curves of rigid biopolymers such as F-actin with contour length comparable to the persistence length as illustrated by Figure 5. In particular, they affect the force regime $f < f_L$. The interpolation formula (C.5) can be compared with exact numerical force-extension curves from transfer matrix calculations for the continuous SHC as described in Section 9. The accuracy of (C.5) is within 10% of the exact curves for a wide range of values $\tilde{L}_{\rm p}/L$ as demonstrated in Figure 5.

Appendix C.2. Extensible SHC

For an *extensible* SHC for forces $f \gg f_{k,\rm cr}$ we have further corrections arising from the overall elastic response of a chain with finite stretching modulus k [14] at strong stretching and from the coupling of thermally fluctuating elastic bonds to the external force. It is no longer possible to include these corrections, as given in (40) for strong stretching and (48) for weak stretching, in reasonably simple explicit interpolation formulae. Starting from our above interpolation formula (C.4) for the inextensible SHC we can only construct an implicit interpolation formula that has to be solved for forces f numerically. The corrections due to extensibility can be incorporated into (C.4) in the following way:

$$\begin{aligned}\frac{f}{f_{\rm cr}} = \frac{1}{2B}&\left[\left(1+\frac{d_\perp^2}{4}\frac{Bf_2(\epsilon_f)}{(1-\ell_f+\epsilon_f)^2}\right)^{1/2}\right. \\ &\left.-\left(1+\frac{d_\perp^2}{4}\frac{Bf_2(\epsilon_f)}{(1+\epsilon_f)^2}\right)^{1/2}\right] \\ &+\frac{d_\perp}{4}\frac{L_{\rm p}}{L}f_1(\epsilon_f)\left(\frac{1}{1-\ell_f+\epsilon_f}-\frac{1}{1+\epsilon_f}\right) \\ &+\left(-\frac{d_\perp^2}{8}\left(1+\frac{d_\perp^2}{4}B\right)^{-1/2} - \frac{d_\perp}{4}\frac{L_{\rm p}}{L}\right. \\ &\left.+\frac{d(d-1)}{4}\frac{1}{\mathcal{L}\left(\tilde{L}_{\rm p}/L\right)}\right)\ell_f\end{aligned} \tag{C.7}$$

with $\epsilon_f \equiv f/f_k$ as the relative extension of an individual bond stretched with a force f and functions $f_1(x) \equiv (1+2x)/(1+x)$ and $f_2(x) \equiv (1+2x)^2/(1+x)$. To keep expression (C.7) reasonably simple we assumed that $f_k \gg f_{\rm cr}$, see (27), and neglected all extensibility effects in the weak-stretching regime where f is linear in ℓ_f. Again we can consider two limiting cases. For $B \ll 1$ effects from the discrete chain structure can be neglected and (C.7) reduces to

$$\begin{aligned}\frac{f}{f_{\rm cr}} = &\frac{d_\perp^2}{16}f_2(\epsilon_f)\left(\frac{1}{(1-\ell_f+\epsilon_f)^2}-\frac{1}{(1+\epsilon_f)^2}\right) \\ &+\frac{d_\perp}{4}\frac{L_{\rm p}}{L}f_1(\epsilon_f)\left(\frac{1}{1-\ell_f+\epsilon_f}-\frac{1}{1+\epsilon_f}\right) \\ &+\left(-\frac{d_\perp^2}{8} - \frac{d_\perp}{4}\frac{L_{\rm p}}{L} + \frac{d(d-1)}{4}\frac{1}{\mathcal{L}\left(\tilde{L}_{\rm p}/L\right)}\right)\ell_f\,.\end{aligned} \tag{C.8}$$

If we also consider the limit of an infinite chain $L_{\rm p} \ll L$ we obtain

$$\begin{aligned}\frac{f}{f_{\rm cr}} = &\frac{d_\perp^2}{16}f_2(\epsilon_f)\left(\frac{1}{(1-\ell_f+\epsilon_f)^2}-\frac{1}{(1+\epsilon_f)^2}\right) \\ &+\frac{d^2-1}{8}\ell_f\,.\end{aligned} \tag{C.9}$$

The interpolation formulae (C.7), (C.8), and (C.9) for the extensible SHC are of the form $f = F(f, L_f)$ with a function F that contains all force scales as fitting parameters. Although they are implicit as the force f appears also on the r.h.s., the following procedure can be used to fit experimental force-extension curves. The implicit or self-consistent force-extension relation $f = F(f, L_f)$ can be formally converted into an explicit formula by replacing f by a formally independent force $\tilde{f}$ on the r.h.s., *i.e.*, $f = F(\tilde{f}, L_f)$. Then we have to fulfill an additional self-consistency condition $\tilde{f} = f(L_f)$ along the actual force-extension curve $f(L_f)$. In this form the interpolation formulae can be used to fit force-extension data, that also has to be extended to include data for $\tilde{f}$. Using identical data for f and $\tilde{f}$, *i.e.*, setting $\tilde{f} \equiv f$ in the experimental data, we will obtain fits that fulfill the required self-consistency condition $\tilde{f} = f(L_f)$ to a good approximation along the actual force-extension curve.

The effects of the extensibility on the force-extension curves are illustrated in Figure 5 Also for the extensible SHC the finite-size effects described by (C.7) or (C.8) lead to pronounced corrections in the force-extension curves in the whole regime $L_f/L < 1$. The interpolation formula (C.8) can be compared with exact numerical force-extension curves from transfer matrix calculations for the continuous SHC as described in Section 9. The accuracy of (C.8) is within 10% of the exact curves for a wide range of values $\tilde{L}_\mathrm{p}/L$ as demonstrated in Figure 5.

References

1. O. Kratky, G. Porod, Recl. Trav. Chim. **68**, 1106 (1949).
2. R.A. Harris, J.E. Hearst, J. Chem. Phys. **44**, 2595 (1966).
3. N. Saito, K. Takahashi, Y. Yunoki, J. Phys. Soc. Jpn. **22**, 219 (1967).
4. M. Fixman, J. Kovac, J. Chem. Phys. **58**, 1564 (1973).
5. J. Kovac, C.C. Crabb, Macromolecules **15**, 537 (1982).
6. C. Bustamante, J.F. Marko, E.D. Siggia, S. Smith, Science **265**, 1599 (1995).
7. S. Smith, Y. Cui, C. Butamante, Science **271**, 795 (1996).
8. M. Rief, J.M. Fernandez, H.E. Gaub, Phys. Rev. Lett. **81**, 4764 (1998).
9. T. Hugel, M. Grosholz, H. Clausen-Schaumann, A. Pfau, H. Gaub, M. Seitz, Macromolecules **34**, 1039 (2001).
10. M. Rief, M. Gautel, F. Oesterhelt, J.M. Fernandez, H.E. Gaub, Science **276**, 1109 (1997).
11. X. Liu, G.H. Pollack, Biophys. J. **83**, 2705 (2002).
12. J.F. Marko, E.D. Siggia, Macromolecules **28**, 8759 (1995).
13. P. Cluzel, A. Lebrun, R. Lavery, J.-L. Viovy, D. Chatenay, F. Caron, Science **271**, 792 (1996).
14. T. Odijk, Macromolecules **28**, 7016 (1995).
15. M.D. Wang, H. Yin, R. Landick, J. Gelles, S.M. Block, Biophys. J. **72**, 1335 (1997).
16. C. Bouchiat, M.D. Wang, J.-F. Allemand, T. Strick, M. Block, V. Croquette, Biophys. J. **76**, 409 (1999).
17. R.R. Netz, Macromolecules **34**, 7522 (2001).
18. L. Livadaru, R.R. Netz, H.J. Kreuzer, Macromolecules **36**, 3732 (2003).
19. B. Maier, U. Seifert, J.O. Rädler, Europhys. Lett. **60**, 622 (2002).
20. R.G. Winkler, J. Chem. Phys. **118**, 2919 (2003).
21. M. Doi, S.F. Edwards, *The Theory of Polymer Dynamics* (Oxford University Press, New York, 1986) p. 316.
22. B.-Y. Ha, D. Thirumalai, J. Chem. Phys. **106**, 4243 (1997).
23. A. Lamura, T.W. Burkhardt, G. Gompper, Phys. Rev. E **64**, 061801 (2001).
24. K. Kroy, E. Frey, Phys. Rev. Lett. **77**, 306 (1996).
25. H. Kleinert, *Path Integrals in Quantum Mechanics, Statistics and Polymer Physics* (World Scientific, Singapore, 1995) pp. 370 and 590.
26. Alternatively $\tilde{L}_\mathrm{p} = 2\kappa/(d-1)T$, which includes the dimension-dependent factor $1/(d-1)$, is used as definition of the persistence length in the literature. We use the dimension-independent definition $L_\mathrm{p} = 2\kappa/T$ in this paper.
27. P.J. Flory, *Statistical Mechanics of Chain Molecules* (Interscience, New York, 1969).
28. A. Ott, M. Magnasco, A. Simon, A. Libchaber, Phys. Rev. E **48**, (1993) R1642.
29. W.H. Taylor, P.J. Hagerman, J. Mol. Biol. **212**, 363 (1990).
30. P. Janmey, J.X. Tang, C.F. Schmidt, *Actin filaments* in *Biophysics Textbook online*, `http://www.biophysics.org/btol/`.
31. R.P Feynman, A.R. Hibbs, *Quantum Mechanics and Path Integrals* (McGraw-Hill, 1995).
32. V. Sa-yakanit, C. Kunsombat, O. Niamploy, *Path Integral Approach to a Single Polymer Chain with Excluded Volume Effect*, in *Biological Physics 2000* (World Scientific, Singapore, 2001).
33. M. Abramowitz, A.I. Stegun, *Handbook of Mathematical Functions* (Natl. Bur. Stand., Washington, 1965).
34. E.M. Lifshitz, L.D. Landau, *Theory of Elasticity* (Pergamon Press, New York, 1986).